ABSTRACT

ARQ PROTOCOL FOR JOINT SOURCE AND CHANNEL CODING AND ITS APPLICATIONS

by
Bin He

Shannon's separation theorem states that for transmission over noisy channels, approaching channel capacity is possible with the separation of source and channel coding. Practically, the situation is different. Infinite size blocks are needed to achieve this theoretical limit. Also, time-varying channels require a different approach. This leads to many approaches for source and channel coding. This dissertation will address a joint source and channel coding that suits Automatic Repeat Request (ARQ) application and applies it to packet switching networks. Following aspects of the proposed joint source and channel coding approach will be presented:

1. The design of the proposed joint source and channel coding scheme. The approach is based on a variable length coding scheme which adapts the arithmetic coding process for joint source and channel coding.

2. The protocol using this joint source and channel coding scheme in communication systems. The error recovery technique of the proposed scheme is presented.

3. The application of the scheme and protocol. The design is applied to wireless TCP network and real-time video transmissions.

The coding scheme embeds the redundancy needed for error detection in source coding stage. The self-synchronization property of lossless compression is utilized by decoder to detect channel errors. With this approach, error detection may be

delayed. The delay in detection is referred to as error propagation distance. This work analyzes the distribution of error propagation distance. The error recovery technique of this joint source and channel coding for ARQ (JARQ) protocol is analyzed. Throughput is studied using signal flow graph for both independent channel and nonindependent channels. A packet combining technique is presented which utilizes the non-uniform distribution of error propagation distance to increase the throughput.

The proposed scheme may be applied to many areas. In particular, two applications are discussed. A TCP/JARQ protocol stack is introduced and the coordination between TCP and JARQ layers is discussed to maximize system performance. By limiting the number of retransmission, the proposed scheme is applied to real-time transmission to meet timing requirement.

ARQ PROTOCOL FOR JOINT SOURCE AND CHANNEL CODING AND ITS APPLICATIONS

by
Bin He

A Dissertation
Submitted to the Faculty of
New Jersey Institute of Technology
in Partial Fulfillment of the Requirements for the Degree of
Doctor of Philosophy in Electrical Engineering

Department of Electrical and Computer Engineering

August 2001

APPROVAL PAGE

ARQ Protocol for Joint Source and Channel Coding and Its Applications

Bin He

Dr. Constantine N. Manikopoulos, Dissertation Advisor   Date
Associate Professor of Electrical and Computer Engineering, NJIT

Dr. Yun-Qing Shi, Committee Member   Date
Associate Professor of Electrical and Computer Engineering, NJIT

Dr. Symeon Papavassiliou, Committee Member   Date
Assistant Professor of Electrical and Computer Engineering, NJIT

Dr. Huifang Sun, Committee Member   Date
Deputy Director, Murray Hill Lab, Mitsubishi Electric Research Laboratories

Dr. George F. Elmasry, Committee Member   Date
Member of Technical Staff, Lucent Technologies

BIOGRAPHICAL SKETCH

Author: Bin He

Degree: Doctor of Philosophy

Date: August 2001

Undergraduate and Graduate Education:

- Doctor of Philosophy in Electrical Engineering,
  New Jersey Institute of Technology, Newark, NJ, 2001

- Master of Science in Electrical Engineering,
  Beijing University of Aeronautics and Astronautics, Beijing, P. R. China, 1997

- Bachelor of Engineering in Electrical Engineering,
  Beijing University of Aeronautics and Astronautics, Beijing, P. R. China, 1993

Major: Electrical Engineering

Publications and Presentations:

B. He and C. N. Manikopoulos, "Performance analysis of ARQ protocol with delayed detection for joint source and channel coding," in *Proceedings of the 35th Annual Conference on Information Sciences and Systems*, (Baltimore, MD), Mar. 2001.

B. He and C. N. Manikopoulos, "A comparison between two error detection techniques using arithmetic coding," in *Proceedings of the Data Compression Conference*, (Snowbird, Utah), Mar. 2001.

B. He and C. N. Manikopoulos, "An automatic repeat request protocol using joint source and channel coding," in *Proceedings of the CSCC 2000 World Multi-conference*, (Athens, Greece), July 2000.

B. He, G. F. Elmasry and C. N. Manikopoulos, "A network protocol for joint lossless-source and channel coding (JARQ) with packet combining," in *Proceedings of the 34th Annual Conference on Information Sciences and Systems*, (Princeton, NJ), Mar. 2000.

B. He, G. F. Elmasry, C. N. Manikopoulos, and Y.-Q. Shi, "A Go-Back-$N + 1$ protocol and its application in wireless ATM networks," in *Proceedings of the 33rd Annual Conference on Information Sciences and Systems*, (Baltimore, MD), Mar. 1999.

B. He and C. N. Manikopoulos, "Performance of an ARQ protocol based on joint source and channel coding on nonindependent channel," to appear in *Proceedings of the IEEE Vehicular Technology Conference (VTC-01/Fall)*, (Atlantic City, NJ), Oct. 2001.

B. He and C. N. Manikopoulos, "A comparison between two error detection techniques using arithmetic coding," to appear in *Proceedings of the International Conference on Computing and Information Technologies*, (Upper Montclair, NJ), Oct. 2001.

B. He, G. F. Elmasry and C. N. Manikopoulos, "Joint lossless-source and channel coding using ARQ/Go-Back-(N, M) for image transmission," submitted to *IEEE Trans. Image Processing*, 2000.

B. He and C. N. Manikopoulos, "ARQ protocols for joint lossless-source and channel coding with delayed detection," submitted to *IEEE Trans. Commun.*, 2000.

B. He and C. N. Manikopoulos, "Performance analysis of ARQ protocols for joint lossless-source and channel coding with delayed detection," to be submitted to *IEEE Trans. Commun.*, 2001.

B. He and C. N. Manikopoulos, "Efficient joint source and channel coding ARQ protocol for wireless networks," to be submitted to *Electronic Letters*, 2001.

This work is dedicated to my beloved family

ACKNOWLEDGMENT

First and foremost, I would like to express my sincere gratitude to my Advisor, Prof. Manikopoulos. I feel extremely fortunate to have him as my advisor. I am deeply grateful to him for his valuable suggestions, continuous support and consistent encouragement. His style of guidance and his creativity made my graduate study a great experience.

I extend my sincere appreciation to my dissertation committee, Prof. Yun-Qing Shi, Prof. Symeon Papavassiliou, Dr. Huifang Sun (Murray Hill Lab, Mitsubishi Electric Research Laboratories) and Dr. George F. Elmasry (General Dynamics Communication Systems, formerly Lucent Technologies) for their interest in this work and stimulating discussions and suggestions. I would especially like to acknowledge Dr. Elmasry for his invaluable support and contribution to my professional development.

I have thoroughly enjoyed knowing and working with fellow researchers during my study. I would like to thank my friends in the department, especially Feihong Chen, Qiang Peng, Minyi Zhao and Surong Zeng, for their continuous help and valuable discussions. I also appreciate Ms. Lisa Fitton, wife of Dr. Elmasry, for her help in revising and editing my paper.

Finally, I would like to express my special gratitude to my family. I am very grateful to my parents, Taixiang He and Zhaolan Xie, for their endless love and support. They always have confidence in me. I would like to express my deepest and special gratitude to my wife and closest friend, Min Tan, who provided continuous encouragement and brought so much happiness and joy into my life. Words cannot express the gratitude I feel toward them.

TABLE OF CONTENTS

TABLE OF CONTENTS
(Continued)

Chapter   **Page**

LIST OF FIGURES

Figure   **Page**

CHAPTER 1

INTRODUCTION

1.1 Background and Motivation

The source and channel coding scheme originates in 1948 with Claude Shannon's paper [1], which states that for stationary and memoryless source and channel, if the entropy rate of the source is below the capacity of the channel, then the source can be reliably transmitted through the channel by appropriate encoding and decoding operations. Moreover, the source coding and channel coding can be designed independently without loss of any optimality. By dividing a difficult problem into two simpler ones, this idea, known as the separation theorem, has led to enormous advances in communication theory and application.

However, the use of separation theorem is limited by its ideal assumption. In fact, many communication systems either violate the assumption or operate with the constraints which the separation theorem does not take into account. These systems may be included in following categories.

1. Vembu *et al.* [2] found an information-stable source/channel pair an exception to the separation theorem. In general, the time-varying source and channel in wireless communication systems does not satisfy the theorem.

2. In most systems, source codes are designed assuming that the channel codes can detect or correct all errors, and channels codes are designed assuming that all bits created by the source code are equally important. This equal error protection (EEP) design results in the codes fragile to catastrophic failure, where a single bit error in the compressed data may cause the decoding corrupted [3].

3. Multimedia communication users often share channel resources, such as in the Internet, and require certain quality of service (QoS). A system, ignoring the

constraints and building from separately designed source and channel codes, may require many channel resources and result in big delay to meet the QoS.

As a result, the separation theorem does not hold in these systems and a joint source and channel design is needed to optimize the source and channel codes, especially in the wireless communication systems and the Internet services. Therefore, joint source and channel coding (JSCC) is receiving increasing attention.

Several approaches were studied to design the joint source and channel codes. One approach places a coder between the source and channel coders and allocates fixed rate between them to maximize the system performance [4]. The recent interest in channel optimized vector quantization (COVQ) is also used in JSCC design where a vector quantizer and an associated receiver incorporate the known channel error characteristics. This work includes those of Goldsmith [5] and Kafedziski and Morrell [6] who proposed a design over a frequency selective fading channel. Unequal error protection (UEP) [7], opposed to EEP, is applied to JSCC where the minimum distance between the code word of the most important information is larger than that of the least important information. Morelos-Zaragoza et al. [8] and Isaka et al. [9] discussed the symmetric and asymmetric modulation for UEP, respectively.

While most of the above work describe the JSCC with fixed length codes, JSCC with variable length codes obtains increasing interests in recent research in spite of its potential catastrophic failure due to error propagation [3]. The reason is that variable length codes generally utilize the limited channel resource, e.g., bandwidth, more efficiently. Sayood and Borkenhagen [10] and Sayood et al. [11] presented a JSCC design using the residual redundancy at the output of the source coder. Yang et al. [12] used the self-synchronization property of Huffman code to correct error for image transmission. Boyd et al. [13] introduced redundancy by adjusting the coding space such that some parts are never used by encoder. If decoding process enters the forbidden region, an error must have occurred. Sayir [14] provided a

method to modify source distributions to produce a code word with any information rate, which enables to perform JSCC. Elmasry [15] embedded parity check bits in arithmetic coding for error correction.

Based on the fact that JSCC may intrinsically improve system performance for wireless communication systems and the Internet service, a JSCC scheme with variable length codes using arithmetic coding is proposed. Moreover, one notices that while most of the work of JSCC is done in communication domain, little is carried out in network domain, e.g., in terms of throughput, delay, etc. This work proposes a error recovery technique for the proposed JSCC design (JARQ protocol) and analyzes its throughput on both independent channel and nonindependent channels. Inspired by the rapid development of wireless communication and the Internet, two applications of the proposed JSCC scheme are discussed—a TCP/JARQ protocol stack for wireless TCP networks with data link layer (DLL) using the proposed error recovery technique and a real-time transmission system with limited number of retransmissions to guarantee timing requirements.

While this work utilizes the JSCC design introduced by Elmasry [16], their focuses are totally different. Elmasry [16] concentrated on introducing different marker strategies as redundancy for error recovery and analyzing the file expansion ratio of each strategy. This work goes further by analyzing the error propagation distance probability density function (PDF), introducing a new marker strategy to prevent long error propagation distance, and more importantly, analyzing the performance of error recovery technique and integrating the JSCC design in some important applications.

1.2 Organization of the Dissertation

Chapter 2 presents the coding scheme. In Section 2.1, a JSCC approach is presented that embeds the redundancy needed for error detection in lossless source coding

stage. The source encoder acts also as a channel encoder to save software, hardware and computation time by having a single coding engine that performs both functions. The decoder utilizes the self-synchronization property of lossless compression, e.g., arithmetic coding, to generate indications of errors in the received data.

With the proposed approach, any error pattern is detected and catastrophic error is avoided because of the self-synchronization property. However, the price is that it may introduce error propagation. This is discussed in Section 2.2 with error propagation distance PDF introduced in Section 2.2.1 and modeled in Section 2.2.2. Since the error propagation may cause misdetection, Section 2.3 shows how misdetection happens and presents a scheme to prevent error from propagating too long. A comparison between the proposed JSCC design and others work is discussed in Section 2.4.

The error propagation has both advantage and disadvantage and they are analyzed in Chapter 3. With regard to the disadvantage, Section 3.1 introduces a new ARQ protocol for the proposed JSCC design, JARQ protocol, which accepts a packet only if a certain number of packets that follow it give no indication of error, as well. Though the extra number of retransmissions degrades system performance, the number is usually small so its impact is alleviated.

With regard to the advantage, the non-uniform distribution of error propagation distance is utilized to perform packet combining in Section 3.2 where the decoder has knowledge of the error's location and thus can construct a clean packet from its erroneous retransmissions. This significantly increases throughput, especially when bit error rate (BER) is low.

The performances of JARQ protocol on independent channel and nonindependent channel are analyzed in Chapter 4 and Chapter 5, respectively. The signal flow graph of JARQ protocol is used to calculate the average transmission time and hence the throughput. A nonindependent channel model is also introduced in

Section 5.2. The analysis shows that the JARQ protocol benefits from the large code rate and the packet combining and leads to a better performance. Simulation results in these chapters validate the analysis.

Two applications of JARQ protocol are discussed. In Chapter 6 a TCP/JARQ protocol stack for wireless communication is proposed. The coordination between TCP layer and data link layer using JARQ protocol is discussed to maximize system performance. In Chapter 7, the limited number of retransmissions in JARQ protocol is applied to real-time video transmission to meet the QoS, since the real-time video transmission often can tolerate certain data loss, and timing is the crucial requirement. The delay and delay variance are analyzed for different number of retransmissions.

The final chapter draws some conclusions and discusses future work.

CHAPTER 2

JOINT SOURCE AND CHANNEL DESIGN WITH VARIABLE LENGTH CODES USING ARITHMETIC CODING

The interest of joint source and channel (JSCC) design with variable length codes has considerably increased recently. While many people implemented JSCC with Huffman codes [12], the use of arithmetic code [17–20] is receiving increasing attention because it is more efficient. Boyd *et al.* [13] introduced a JSCC design which adds redundancy by adjusting the coding space of arithmetic codes such that some parts are never used by encoder. If decoding process enters the forbidden region, an error must have occurred. Sayir [14] provided a method to modify source distributions to produce a code word with any information rate, which can enable to perform JSCC. Pettijohn *et al.* [21] presented a design based on the idea of reserving space introduced in [13, 22].

This chapter presents a new JSCC design with variable length codes using arithmetic coding. With the design, "marker" is periodically inserted as redundancy used for error detection. The design is presented in Section 2.1 and delay characteristic is analyzed in Section 2.2. By discussing two types of error propagation, a method to prevent long propagation distance is presented in Section 2.3. Section 2.4 compares the proposed JSCC design and others work, followed by conclusions in final section.

2.1   Joint Source and Channel Design

In the design, lossless-source and channel coding are joined to prevent the source decoder from reconstructing garbled data, while maximizing the achieved throughput. This is achieved by introducing the redundancy needed for error detection to the source data before compression in the form of periodically inserted markers. The decoder examines the reconstructed data for the existence of the inserted markers.

A request for retransmission is generated if a marker does not appear in its proper location [23, 24]. See Figure 2.1.
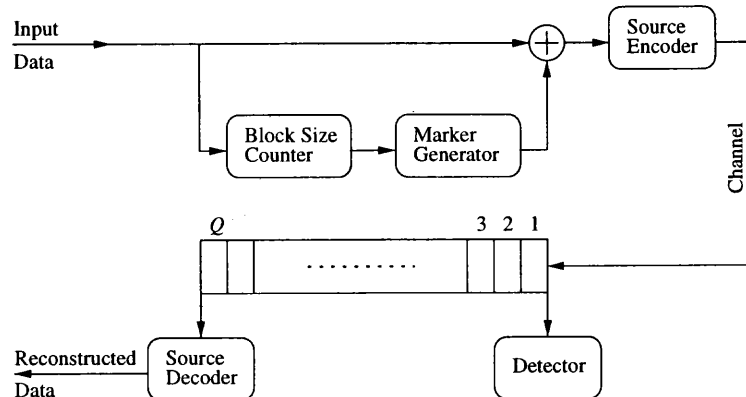
Figure 2.1 Diagram of the JSCC design

Three types of marker strategies were introduced by Elmasry [16], i.e., the particular, the previous and the average marker strategies. The reader can refer to [16] for details about all three marker strategies. This work applies the previous marker strategy, where a block of size m source symbols is turned into a block of size $(m + 1)$ symbols by repeating the mth symbol at the $(m + 1)^{\text{th}}$ location. Also, the ratio of the size of the compressed sequence with the added markers to the size of the compressed sequence without the added markers, i.e., code rate, is $\frac{m}{m+1}$.

Some important features of the proposed JSCC design are summarized below.

1. Clear indication of error propagation at the decoder. When examining the marked blocks, after decompression, the absence of an expected marker denotes the presence of error. However, there is a probability that an error will be misdetected (i.e., the correct marker appears even though an error is present). Nevertheless, as more marker locations are checked, this misdetection probability approaches 0 [16]. That is, even if an error in a packet is misdetected and it will propagate to the packets that follow it, it will eventually be detected. In this manner the decoder can avoid decoding garbled data. This feature will be analyzed in more detail in Section 2.2.

2. Insensitivity to the error pattern. Regardless of the error pattern, the detection capability of the design is the same. This is not the case for conventional system where an error pattern, beyond the detection capability of the channel decoder, will result in garbled data because of the self-synchronization property of the compressed data.

To clarify the notations used for data types in this chapter, the term *symbol* is used to denote an uncompressed source symbol in the original data. *Byte* describes a compressed symbol, and *block* denotes a group of *symbols* plus a marker (uncompressed data) that together form a marked block. *Packet* is the compressed data entity transmitted in the channel. A packet typically decompresses to several *blocks*.

2.2 Delay Characteristic Analysis

2.2.1 Misdetection Probability and Error Propagation Distance

When the channel in Figure 2.1 introduces an error to a compressed byte, the error may not be reflected instantly in the corresponding reconstructed marked block. This delayed detection depends on many factors including the source coding method used, the compression ratio, the marker strategy and the length of the marked block. Because the channel error causes the reconstructed data to be garbled, the error will be detected in the marked blocks that follow it. One will refer to the misdetection probability of checking one marker as P_{mis}. With packet switching networks, data is transmitted in the form of packets and one packet can decompress to l marked blocks. In [16], it was shown that the misdetection probability after checking l markers, $P_{MIS}(l)$, approaches 0 as more data (packets) are received and decompressed, i.e., more markers are checked.

In this work, studying the characteristics of this delayed detection is of interest. This delay will be measured by considering the distance an error may propagate before being detected. This distance is measured in terms of the number

of compressed bytes (starting from the symbol where the error occurred) needed to decompress before the error is detected. Different types of source data are examined, and they can be divided into two categories. The first category is low compression ratio sources (the amount of redundancy to be removed by the source encoder is small). An example of these sources is plain English text files with a compression ratio of $R \approx 1.47$. The second category is high compression ratio sources (the amount of redundancy to be removed by the source encoder is high). An example of these sources is most image files (e.g., for the 256×256 LENA image, the compression ratio $R \approx 6.30$). The source coding method used here is the adaptive arithmetic coding scheme published in [25]. In this work, the delay distance is measured using a simulation program that checks how far an erroneous byte travels in the receiver's buffer in Figure 2.1 before the decompressed data shows the absence of the marker (the error is detected). Statistics are collected for this error propagation distance (in bytes) and a simulation probability density function (PDF) is obtained. This PDF is measured for different marked block lengths ($m = 10, 20$, and 30 for text and image files). The obtained PDF's are shown in Figure 2.2 and Figure 2.3 respectively. Notice that the delay fades much more quickly for a small compression ratio (text files) than for a large compression ratio (image files). A small marked block length m also reduces error propagation, but at the price of decreasing the code rate.

2.2.2 Modeling of Error Propagation PDF

Since the error propagation distance PDF's in Figure 2.2 and Figure 2.3 are different, their misdetection probabilities, $P_{MIS}(l)$, are in turn different. $P_{MIS}(l)$ can be determined by integrating the error propagation PDF with respect to the number of markers checked, instead of the number of compressed bytes which the error travels. Since a mark is inserted every m symbols, $m + 1$ symbols form a marked block, which corresponds to $\frac{m+1}{R}$ compressed bytes (where R is the compression ratio). By
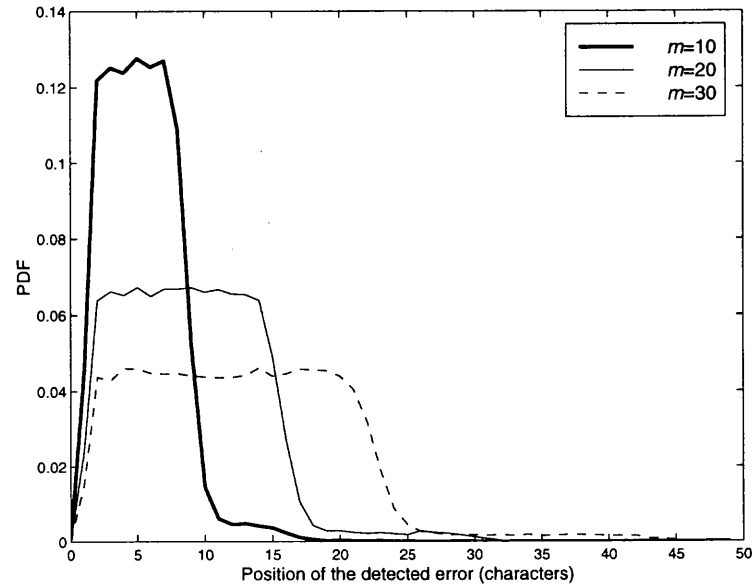
Figure 2.2 Error propagation distance PDF of text transmission
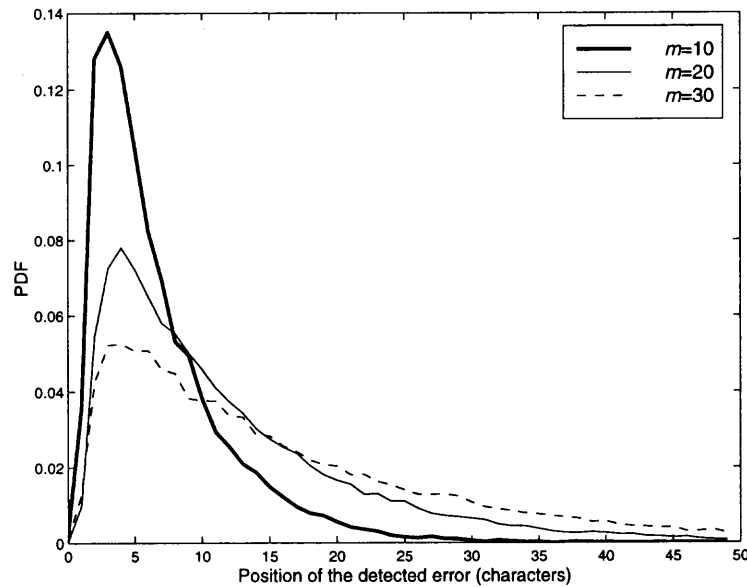
Figure 2.3 Error propagation distance PDF of image transmission

defining error propagation PDF and its cumulative distributed function (CDF) as $f(x)$ and $F(x)$ respectively, one can find the misdetection probability of checking l markers,

$$P_{MIS}(l) = 1 - F\left(\frac{m+1}{R}l\right), \tag{2.1}$$

and the misdetection probability of checking one marker,

$$P_{mis} = P_{MIS}(1) = 1 - F\left(\frac{m+1}{R}\right). \tag{2.2}$$

The goal here is to find $P_{MIS}(l)$ through P_{mis}. For English text files, P_{mis} was found to be $P_{mis} \approx 0.0268$ [16]. Since the error propagation distance is short with text files, $P_{MIS}(l) \approx P_{mis}^l$ is an acceptable approximation. This approximation is shown in Figure 2.4 where $P_{mis} \approx 0.0268$ and $R \approx 1.47$. A marked block length of 21 characters is used (20 source symbols plus one marker). On the average, approximately 14.3 bytes should produce a block with one marker location (21 characters/1.47 $\approx$ 14.3 bytes). With these 14.3 bytes, the probability that a byte decompresses to a marker is $\frac{1}{14.3} \approx 0.07$. Also, the probability that this marker character will indicate the error is $1 - P_{mis}$. If considering on average, the first 14.3 bytes in the receiver's buffer will produce the first marker, and the second 14.3 bytes will produce the second marker, etc., then the error may be detected by one of the first 14.3 bytes with a probability of $0.07(1 - P_{mis})$, while for the second 14.3 bytes the detection probability is $0.07P_{mis}(1 - P_{mis})$, and for the third 14.3 bytes it is $0.07P_{mis}^2(1 - P_{mis})$, etc. This is shown in the dashed line in Figure 2.4, which implies that $P_{MIS}(l) \approx P_{mis}^l$.

However, for image files (and generally for sources with large R), a different approximation is needed. One can see from Figure 2.5 that the PDF fades slowly, and thus the misdetection probability does not attenuate to the order of the number of checked markers. By examining these PDF's, the following approximation is reached,

$$f(x) = a\,x^c e^{-b\,x^d}, \tag{2.3}$$
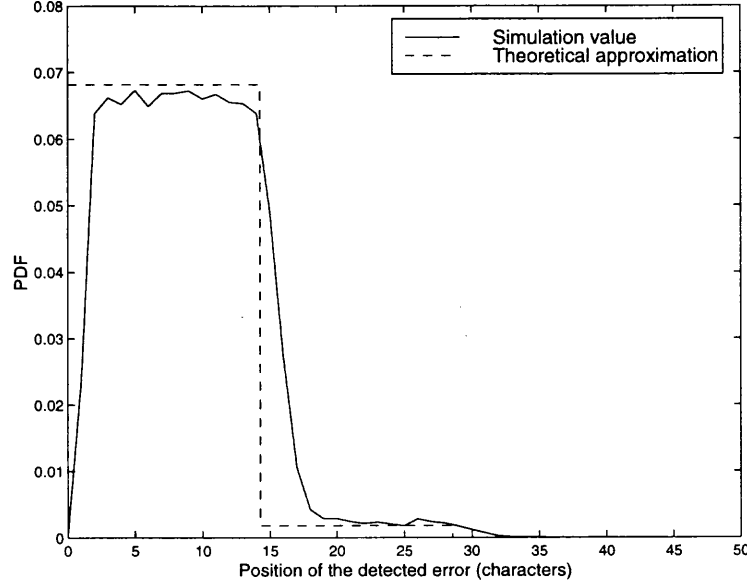
Figure 2.4 Modeling of error propagation PDF for text transmission

where $x = \frac{m+1}{R}l$. A parameter matching program for the above nonlinear function can be found in [26] to determine a, b, c and d. Figure 2.5 shows this approximation for $m = 20$. The parameters a, b, c and d were selected to bound the mean square error between the two curves to less than 1%.

Considering that $F(x) = \int_0^x f(t)\,dt$ and using Eq.(2.3), one can obtain

$$F(x) = \int_0^x a\,t^c e^{-b\,t^d}\,dt. \tag{2.4}$$

Setting $y = t^d$ yields $t^c = y^{c/d}$ and $dt = \frac{1}{d}\,y^{(1-d)/d}\,dy$. Eq.(2.4) becomes

$$F(x) = \int_0^{x^d} \frac{a}{d}\,y^{\frac{1+c-d}{d}}\,e^{-by}\,dy. \tag{2.5}$$

Normally, for an allowable tolerance, it is possible to find the values of c and d to meet $\frac{1+c-d}{d}$ is an integer, denoted as u. Eq.(2.5) becomes

$$
\begin{aligned}
F(x) &= \frac{a}{d}\int_0^{x^d} y^u e^{-by}\,dy \\
&= \frac{a}{d}\left(-\frac{e^{-by}}{b^{u+1}}\left[(by)^u + u(by)^{u-1} + u(u-1)(by)^{u-2} + \cdots + u!\right]\Big|_0^{x^d} \right) \\
&= \frac{a}{d\,b^{u+1}}\left\{ u! - e^{-bx^d}\left[(bx^d)^u + u(bx^d)^{u-1} + u(u-1)(bx^d)^{u-2} + \cdots + u!\right] \right\}.
\end{aligned}
$$

$$\tag{2.6}$$
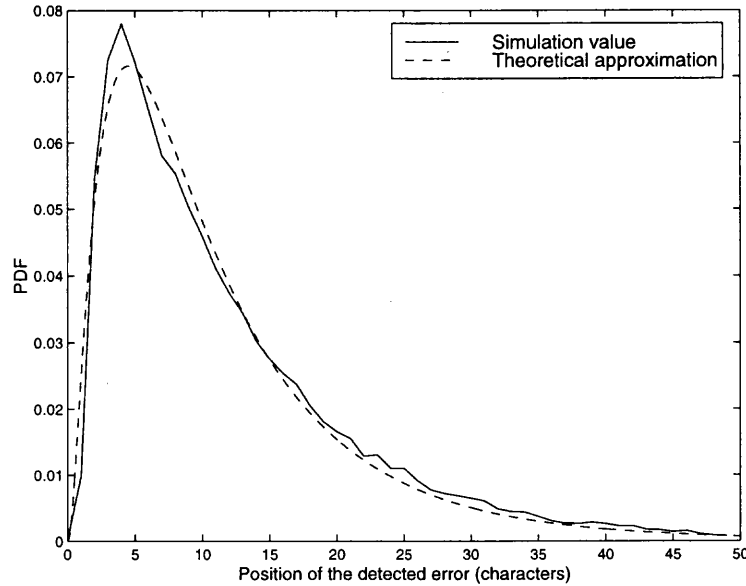
Figure 2.5 Modeling of error propagation PDF for image transmission

Thus, $P_{MIS}(l)$ is derived from Eq.(2.2) and Eq.(2.6) for image files,

$$P_{MIS}(l) = 1 - F\left(\frac{m+1}{R}l\right)$$

$$= 1 - \frac{a}{d\,b^{u+1}}\left\{u! - e^{-bx^d}\left[(bx^d)^u + u(bx^d)^{u-1} + u(u-1)(bx^d)^{u-2} + \cdots + u!\right]\right\}(2.7)$$

where $x = \frac{m+1}{R}l$ and $u = \frac{1+c-d}{d}$.

2.3   Prevention of Long Propagation Distance

2.3.1   Two Types of Error in Arithmetic Coding

Section 2.2 discusses the effect of marker strategy and compression ratio on the error propagation distance. The delay characteristic may also depend on the arithmetic coding algorithm used. To explain this, the arithmetic encoding algorithm is discussed:

1. A current encoding interval is divided into subintervals, one for each possible source symbol and the size of a symbol's subinterval is proportional to its estimated possibility.

2. The subinterval corresponding to the symbol that actually occurs is selected to be the current interval and above operations are repeated.

3. The code word is the enough bits to distinguish the final current interval from all other possible final intervals.

4. The decoding algorithm behaves reversely, recovering source sequence by successively locating the intervals which contains the fraction represented by the code word [25]. See Figure 2.6.
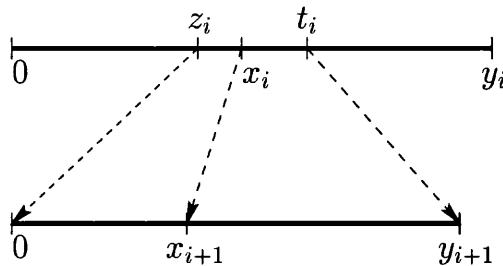
Figure 2.6 Arithmetic decoding algorithm

In Figure 2.6, $[0, y_i)$ is current interval when decoding i^{th} symbol. The information of the symbol's estimated probability is included in x_i. To find the symbol's value, two variables are calculate:

$$z_i = \left\lfloor \frac{F_k}{total_i} \times y_i \right\rfloor \tag{2.8}$$

$$t_i = \left\lfloor \frac{F_{k+1}}{total_i} \times y_i \right\rfloor, \tag{2.9}$$

for $0 \leq k < s$ where s is size of source alphabet. F_k is cumulative frequency to symbol with value k and $total_i$ is number of symbols already decoded. $\lfloor x \rfloor$ is the largest integer less than or equal to x. A symbol with value of k is decoded if and only if

$$z_i \leq x_i < t_i. \tag{2.10}$$

After that current interval is changed to $y_{i+1} = t_i - z_i$ and $x_{i+1} = x_i - z_i$ plus the information of next encoded output. x_{i+1} and y_{i+1} are often scaled to ensure the calculation precision.

If error happens, x_i becomes incorrect, e.g., $\hat{x}_i$. After decoding the ith symbol, there are two types of error:

1. $\hat{x}_{i+1}$ is incorrect. This kind of error is not harmful since the current interval is erroneous after i^{th} symbol, the decoding results get corrupted almost instantly. Thus the previous marker strategy is capable of detecting this type of error.

2. $\hat{x}_{i+1}$ and $\hat{y}_{i+1}$ are correct. In this case, the ith symbol must be decoded incorrectly. Figure 2.7 illustrates how this happens.
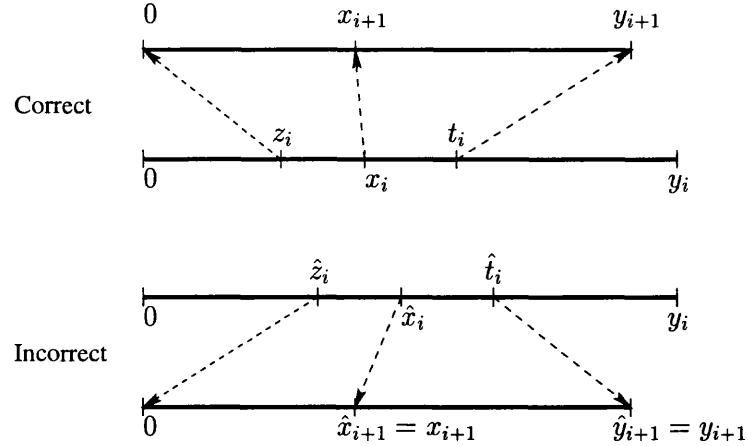
Figure 2.7 Illustration of second type of error

For the second error type, following two variables are calculated:

$$\hat{x}_{i+1} = \hat{x}_i - \hat{z}_i = \hat{x}_i - \left\lfloor \frac{F_{\hat{k}}}{total_i} \times y_i \right\rfloor \tag{2.11}$$

$$\hat{y}_{i+1} = \hat{t}_i - \hat{z}_i = \left\lfloor \frac{F_{\hat{k}+1}}{total_i} \times y_i \right\rfloor - \left\lfloor \frac{F_{\hat{k}}}{total_i} \times y_i \right\rfloor = \left\lfloor \frac{f_{\hat{k}+1}}{total_i} \times y_i \right\rfloor + \hat{\Delta}, \tag{2.12}$$

where $f_{\hat{k}+1}$ is the frequency of symbol $\hat{k}+1$ in frequency table, and $\hat{\Delta}=0$ or 1. If $\hat{x}_{i+1}=x_{i+1}$ and $\hat{y}_{i+1}=y_{i+1}$, one obtains

$$x_i - \hat{x}_i = \left\lfloor \frac{F_k}{total_i} \times y_i \right\rfloor - \left\lfloor \frac{F_{\hat{k}}}{total_i} \times y_i \right\rfloor \qquad (2.13)$$

$$\left\lfloor \frac{f_{k+1}}{total_i} \times y_i \right\rfloor + \Delta = \left\lfloor \frac{f_{\hat{k}+1}}{total_i} \times y_i \right\rfloor + \hat{\Delta}, \qquad (2.14)$$

where $\Delta = 0$ or 1. This means, if the difference caused by the error equals to the distance difference calculated in the current interval (first condition), and the difference between frequency of the symbol with correct value and that of the symbol with incorrect value is not larger than 1 (second condition), the second type of error occurs.

An example of this type of error is when the error occurs in the first encoded byte. The adaptive encoding algorithm is applied and it assigns an initial weight of 1 to each alphabet symbol and add 1 for each occurrence. $total_1$ and y_1 are initialized to s. $f_k = 1$, $F_k = k$ and $F_{\hat{k}} = \hat{k}$ for every k and $\hat{k}$ make the two conditions true. This means the first encoded output should be extra protected.

This type of error is more harmful than the first type since the current interval is correct, the next incorrect symbol cannot be decoded until the incorrect part of frequency table that is caused by the error is used and the impact of this incorrectly decoded symbol to the frequency table accumulates high enough. The decoder will generate a long run of correct symbols between two incorrect symbols. If the first error cannot be detected (e.g., by previous marker strategy), a long error propagation distance will occur. Simulation result shows this kind of error occurs with probability around 10^{-5}.

To cope with this type of error and also reduce the redundancy, since the second error type happens much less frequently than the first type, a block length is selected such that it is much larger than the previous marker strategy's block length, and a marker is added such that its value equals to: (sum value of all symbols in the

block) mod. (s). This approach is called sum marker strategy and it is used with previous marker strategy to detect the error. The probabilities of two types of error can be derived by integrating the possibilities for them to happen according to their frequency in the frequency table.

2.3.2 Experiments

The previous marker strategy is used in the experiments. For a marker block length m, the percentage of file expansion is $\frac{1}{m}$. Elmasry [16] indicated that using an arbitrary value of marker may incur a large file expansion, i.e., large redundancy. This, along with the fact that the second type of error occurs much less frequently, necessitates that the marker block length of sum marker strategy should be chosen large.

The adaptive coding is used, e.g., algorithm proposed by Jones [25], which assigns an initial weight of 1 to each alphabet symbol and add 1 for each occurrence. Let s be the size of source alphabet, n_i the number of occurrences of ith symbol in the alphabet, and l the length of source data. This implies that $\sum_{i=1}^{s} n_i = l$. The code length, before adding any kind of detection strategy, is

$$L_1 = -\log_2 \frac{\prod_{i=1}^{s} n_i!}{s(s+1)\cdots(s+l-1)}. \tag{2.15}$$

Applying the previous and sum marker strategies, the block lengths for them are m_1 and m_2 ($m_1 < m_2$), respectively, and the source data length becomes $l + \frac{l}{m_1} + \frac{l}{m_2}$. The number of ith symbol in the alphabet becomes $n_i + \frac{n_i}{m_1} + \frac{l}{m_2}p_i$, where p_i is the probability that sum marker is the ith symbol in the alphabet. $\frac{n_i}{m_1}$ and $\frac{l}{m_2}p_i$ are the number of added marker by previous and sum marker strategy, respectively. The code length after applying previous and sum marker strategy (i.e., combined

strategy) is,

$$L_2 = -\log_2 \frac{\prod_{i=1}^{s} \left[n_i(1 + \frac{1}{m_1}) + \frac{l}{m_2}p_i \right]!}{s(s+1)\cdots(s+l+\frac{l}{m_1}+\frac{l}{m_2})}. \qquad (2.16)$$

$\frac{L_2 - L_1}{L_1}$ gives the redundancy added by the combined scheme.

The comparison of the combined strategy and the previous marker strategy is based on same amount of redundancy. 256×256 LENA is used as source file. Simulation shows the combined strategy with $m_1 = 40$ and $m_2 = 800$ has similar redundancy to the previous marker strategy with $m_1 = 35$. Their PDFs of error propagation distance are shown in Figure 2.8.
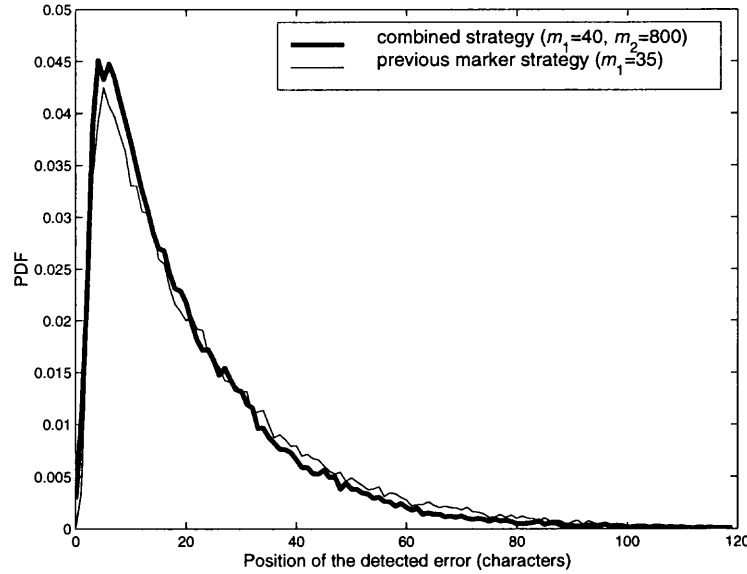
Figure 2.8 Error propagation distance PDF of combined strategy and previous marker strategy

One can see that the combined strategy has a better PDF than previous marker strategy. (The number with smaller propagation distances is more). Moreover, what is not shown in the figure is that the previous marker strategy has several samples with large propagation distance (> 200), but most of them are detected in a small delay by the combined strategy. This means the combined strategy has better

delay characteristic and in turn, less redundancy and larger throughput obtained in communication networks.

2.4   A Comparison Between Two Error Detection Techniques Using Arithmetic Coding

2.4.1   Forbidden Symbol Approach and Marker Symbol Approach

Of the joint source and channel coding using variable length codes, Boyd *et al.* [13] proposed a detecting approach which introduces redundancy by adjusting the coding space such that some parts are never used by encoder. If decoding process enters the forbidden region, an error must have occurred. This approach is called forbidden symbol approach and it is widely used. Kozintsev *et al.* [22] analyzed the performance of this approach in communication system by introducing "continuous" error detection. The redundancy versus error detection time was studied. Pettijohn *et al.* [21] extended this work in sequential decoding to provide error correction capability. Another idea of using arithmetic codes for error detecting was proposed by Elmasry [16] and extended in this chapter, where the redundancy needed for error detection is introduced to the source data before compression in the form of periodically inserted markers. The decoder examines the reconstructed data for the existence of the inserted markers. An error is indicated if a marker does not appear in its proper location.

Two approaches are referred to as forbidden symbol approach and marker symbol approach, respectively. Next section compares the error detection capability of these two approaches in terms of redundancy and error propagation distance (i.e., error detecting time in [22]), which mainly determine the performance of system based on the approach. The comparison shows that while two approaches basically have the same error detection capability, they should be applied to different kind of systems [27, 28].

2.4.2 Comparison of Redundancy and Error Propagation Distance

For forbidden symbol approach, the redundancy and error propagation distance are analyzed by Kozintsev et $al.$ [22], where the forbidden symbol is assigned probability ϵ ($0 < \epsilon < 1$). A random variable $Y1$ with geometric distribution is modeled to represent the number of symbols it takes to detect an error after it occurs, i.e., error propagation distance:

$$P_{y1}(k) = (1 - \epsilon)^{k-1} \epsilon \qquad k = 1, 2, \ldots, \infty, \tag{2.17}$$

and the probability that error propagates more than n symbols decreases with n^{th} order of $(1 - \epsilon)$:

$$P_1[Y1 > n] = (1 - \epsilon)^n. \tag{2.18}$$

The redundancy is

$$R_1 = -\log_2(1 - \epsilon) \qquad \text{bits per symbol.} \tag{2.19}$$

For the marker symbol approach, the previous marker strategy is used (the combined marker strategy described in Section 2.3 has similar or a little better delay characteristics). With the previous marker strategy, a block of size m source symbols is turned into a block of $m + 1$ symbols by repeating the mth symbol at the $(m + 1)^{\text{th}}$ location. Thus the amount of redundancy is

$$R_2 = \frac{1}{m}. \tag{2.20}$$

The PDF remains almost constant in each marker region in Figure 2.2. But between these marker regions, PDF drops quickly. The probability that error is checked within l markers can be statistically determined by simulation. Here an approximation simply explains the result. Assuming one symbol contains c bits, 2^c symbols are in the alphabet. Since even a single error will cause the decoding process losing self-synchronization property and the decoded data being garbled,

when comparing the marker and the previous symbol, the probability that they are the same roughly equals to the probability that two independent numbers selected from 1 to 2^c are same, which is $\frac{2^c}{2^c \times 2^c} = 2^{-c}$. Letting random variable $Y2$ represent number of markers that error propagates, the probability that error propagates more than l markers, i.e., the misdetection probability, is,

$$P_2[Y2 > l] = \left(2^{-c}\right)^l = 2^{-lc}. \tag{2.21}$$

The comparison of the redundancy and error propagation distance between two approaches is based on same amount of redundancy. If the redundancy of marker symbol approach is counted in number of bits per symbol, $R_2 = \frac{c}{m}$ bits are in one symbol. For the same amount of redundancy, $R_1 = R_2$ yields

$$-\log_2(1 - \epsilon) = \frac{c}{m}, \tag{2.22}$$

or,

$$(1 - \epsilon)^m = 2^{-c}. \tag{2.23}$$

This means the probability that error propagates more than m symbols in forbidden symbol approach is equal to the probability that error propagates more than 1 marker in marker symbol approach. Similarly for l markers, $(1-\epsilon)^{lm} = 2^{-lc}$ is obtained. This means two approaches have basically the same error detection capability. Figure 2.9 compares two approaches with same redundancy. The forbidden space $\epsilon = 0.12$ and marked block size $m = 30$ are selected. Two approaches have different error propagation distance PDF, but for error that propagates beyond a marked block size, the detection probabilities are same (the areas of two curves in each marked block size are same).

However, with the forbidden symbol approach, the error propagation distance distribution is non-uniform. This makes the approach useful in the cases which require error correction. The reason is that one can estimate the error location from
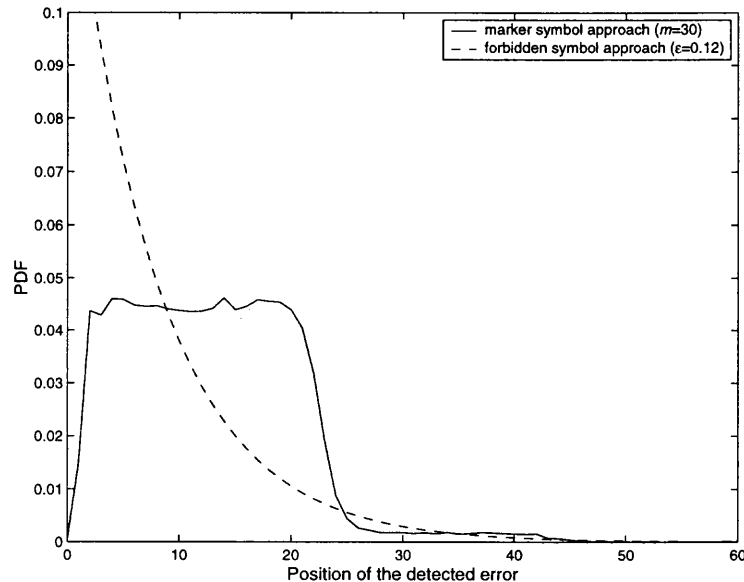
Figure 2.9 Comparison of error propagation distances of two approaches

the geometrically distributed error propagation distance. While in marker symbol approach, the error location PDF within a marked block is approximately uniformly distributed. One can only guess the error in terms of marked block, but does not know the error position within the block.

Although the marker symbol approach is less efficient in error correction, it is simple and does not change the entropy code in encoder and decoder. The approach can be applied to existing systems without modification of encoder and decoder. Moreover, though forbidden symbol approach provides continuous error detection, in current packet switching networks there is no need for high frequency of error checking. By introducing several markers in a packet, the marker symbol approach is capable of detecting errors with less computation complexity.

2.5 Conclusion

In this chapter, a JSCC design with arithmetic codes is proposed. The self-synchronization property of arithmetic codes is used to detect error, at the price of introducing error propagation. The error propagation distance PDF is discussed and

modeled for both text and image transmission. The arithmetic coding with adaptive algorithm is discussed and two types of error are found. The first type of error is suitable for previous marker strategy to detect and for the second type of error, a new detection strategy is introduced. Two strategies are combined to detect errors. Simulation result shows that this combined scheme is capable of detecting error with small delay, which gives more code rate and throughput in communication networks.

A comparison of the error detection capability is presented between two error detection approaches with arithmetic coding, i.e., forbidden symbol approach and marker symbol approach. It shows two approaches have basically the same error detection capability. With its geometric distribution of error propagation distance, the forbidden symbol approach is useful in the cases where the error location can be estimated for error correction. The marker symbol approach is simple and does not change the source encoding and decoding design. Though forbidden symbol approach provides continuous error detection, its high frequency of error checking is generally not needed in packet switching networks. The marker symbol approach with less computation complexity may be a better choice in this case.

CHAPTER 3

ERROR RECOVERY PROTOCOL OF THE PROPOSED JOINT SOURCE AND CHANNEL DESIGN

With packet switching networks, error recovery techniques conventionally use Automatic Repeat Request (ARQ) protocols, such as Cyclic Redundancy Codes (CRC). These techniques utilize a channel coding approach that divides the data into blocks of length k bits and adds redundancy to each block to form code words of length n bits. The ratio $\frac{k}{n}$ is referred to as the code rate [29]. The added redundancy $(n - k)$ is utilized by the receiver for error detection. Since compressed data is intolerant to errors, a single unrecovered channel error results in the loss of the self-synchronization property of the compressed data, which causes the reconstructed data to become garbled from the point where the error occurred to the end of the decoded sequence. For conventional ARQ protocols to achieve reliable transmission, they either

1. use an excessive amount of redundancy, which decreases throughput efficiency,

2. increase the code word size, n, which increases the code complexity and the transmission delay, or

3. utilize fixed-length compression techniques, which affects the obtained compression gain and in turn decreases the achieved throughput efficiency.

Therefore, in this chapter, an ARQ protocol using the joint source and channel coding design (JARQ protocol) is introduced in Section 3.1 that utilizes the self-synchronization property of the data compression for the benefit of error recovery. By taking the advantage of nonuniform error propagation distance PDF, packet combining is performed in Section 3.2 to improve system performance.

3.1   Introduction to the JARQ Protocol

With the delay characteristic explained in Section 2.2, error detection may occur because of an error in a previous packet rather than in the current one. To account for this scenario, a modification in the conventional ARQ protocol, e.g., Go-Back-N request for retransmission algorithm [30, 31], was developed. This modified algorithm is called the JARQ protocol and in particular, the Go-Back-(N, M) $(M \geq 1)$ protocol. This protocol accepts a packet only after checking that no errors are detected when decompressing it as well as the M packets that follow it [32–34].

In this analysis, $M + 1$ detection states (state 0 to state M) are defined and the state number stands for the number of packets held at the receiver previous to the current packet. The detection state flow starts from state 0, as shown in Figure 3.1. State i $(1 \leq i \leq M)$ is obtained through receiving i consecutive packets with no error detection. Once an error is detected in a received packet, the detection process returns back to state 0, which means that a retransmission is requested. Upon reaching state M, if no error is detected in the received packet, the earliest held packet will be released, the state will remain unchanged, and a new one will be received. State M is obviously the desired working state.

Detection Success (solid line)

release old and
receive new packet

Detection Failure (dashed line)
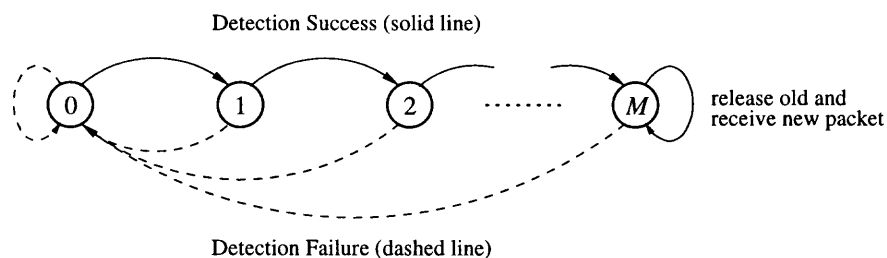
Figure 3.1 Detection state flow of Go-Back-(N, M) $(M \geq 1)$ protocol

When an error is detected, if M is large, a large number of packets have to be retransmitted, which decreases the throughput. On the other hand, a large M is desirable because checking more packets (and as a result more marker locations) reduces the probability of misdetection. As seen in Figure 2.2 and Figure 2.3, errors

normally will not propagate to a large number of bytes. Because a packet contains several blocks, $M = 1$ or 2 can be selected in most applications. This implies small overhead.

Figure 3.2 illustrates this protocol for $M = 1$ with two types of error. In the first type the error is detected within the packet that contains it, and in the second type the error detection is delayed until the next packet. Since it is impossible to know if the error is of the first or second type, an extra packet (before the detected packet) is always retransmitted.
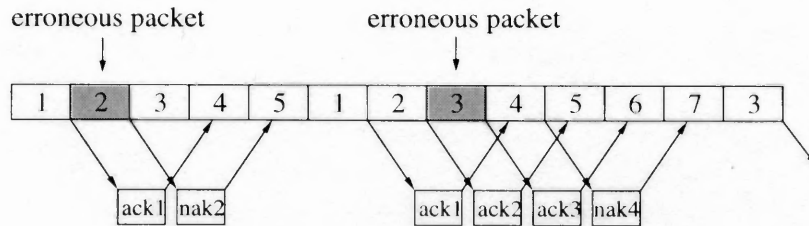
Figure 3.2 Go-Back-(N, M) protocol ($M = 1$)

Notice that on average $(\frac{1}{2} + M)l$ markers are checked after the error, where l is the average number of marked blocks generated when decompressing a packet. Thus, $P_{MIS}(l)$ becomes $P_{mis}^{(\frac{1}{2}+M)l}$ for the small compression ratio case.

Although the misdetection probability is small, in case misdetection occurs, the recovery mechanism employed should depend on the application or service at hand, i.e., garbled data could be dropped; retransmission could be restarted from the beginning of the last file; or the value of M could be chosen adaptively.

3.2 Throughput Enhancement with Packet Combining

With the presented protocols, one can expect that at low BER's, the request for retransmission will occur with less frequency, and thus the effect of the extra M retransmitted packets will be small. Throughput gain can be achieved from increasing the code rate with JARQ protocol. At high BER's the effect of the extra

retransmitted M packets will overcome the gain obtained from increasing the code rate, and JARQ protocol is expected to give less throughput than conventional ARQ protocols. Note, however, that at high BER's, JARQ can be used as the outer code (in a concatenated coding approach), where the inner code is designed for error correction. With this approach, a decoding failure from the inner code produces a burst error. With concatenated codes, interleaving is often used for the outer code. However, if JARQ is to be used as the outer code, interleaving can be avoided since JARQ's error detection capability is not affected by the error pattern.

Also note that with JARQ, the decoder has knowledge of the PDF of the detected error's location, as explained in Chapter 2. This can be utilized to further improve the achieved throughput. With JARQ, instead of performing de-interleaving, the receiver can perform packet combining [35].

Note that when using conventional ARQ protocols, the decoder estimate of the error location PDF is a uniform distribution (since interleaving spreads the error throughout the entire frame and the decoder cannot pinpoint the exact location of the error in each packet). This is not the case with JARQ. With JARQ, if the receiver receives two consecutive noninterleaved frames with error and these two frames represent the same data: one is the original transmission, while the other is the retransmission, a second retransmission can often be avoided. Based on the estimation of the delay PDF in Figure 2.2 and Figure 2.3, the decoder can pinpoint the location of the error in each frame to particular packets with high probability. Then packet combining is performed (where packets with error are dropped from each frame), and the resulting combined frame is decompressed error-free. This significantly increases throughput. Figure 3.3 shows a scenario of this packet combining where the first received frame is decoded, and the absence of the marker pinpoints the location of the error to certain packets according to the estimated PDF (packets marked 1 and 2). With the second copy, the absence of the marker pinpoints the

location of the error to different packets (packets 8 and 9). By replacing packets 1 and 2 in the original transmission by packets 1 and 2 in the retransmission, a second retransmission is avoided.
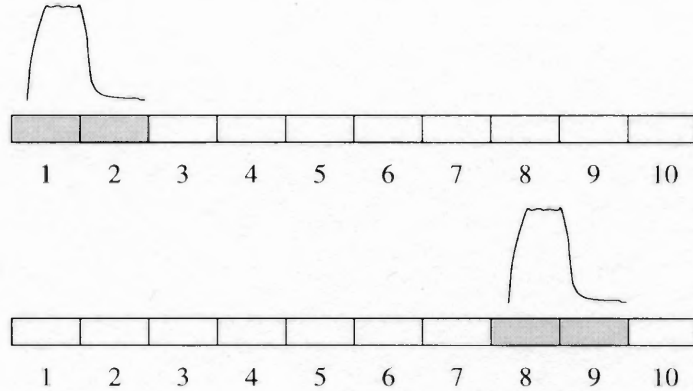
Figure 3.3 Apply packet combining to a frame and its copy

3.3   Summary

An error recovery scheme called JARQ protocol is presented for transmission of compressed data over packet switching networks using the proposed joint source and channel design. Since it is possible that the error detection process encounters some delay, Go-Back-(N, M) protocol is proposed where the receiver accepts the current packet as correct only when the following M packets are correct, as well. Taking the advantage of nonuniform error propagation distance PDF, the receiver can estimate the error location and perform packet combining. A second retransmission is often avoided and system performance is improved.

CHAPTER 4

THROUGHPUT ANALYSIS OF JARQ PROTOCOL ON INDEPENDENT CHANNEL

The previous chapter has introduced a joint source and channel design using arithmetic. Because of the self-synchronization property, a delayed detection error recovery approach, JARQ protocol, is presented. In this chapter, the performance of JARQ protocol on independent channel is analyzed. Section 4.1 introduces signal flow graph to find the average transmission time and hence the throughput. Although the analysis shows the performance is degraded because of extra retransmissions, it can be improved by the large code rate discussed in Chapter 3, or the optimal case in Section 4.2, or the packet combining in Section 4.3. Simulation results in Section 4.4 show the performance and validate the analysis.

4.1 Throughput Analysis of Go-Back-(N, M) Protocol

The signal flow graph is used to derive the performance of JARQ protocol. A signal flow graph [36, 37] is a diagram which represents a set of simultaneous equations. It consists of a graph in which nodes are connected by directed branches. The nodes represent each of the system variables. A branch connected between two nodes acts as a one-way signal multiplier: the direction of signal flow is indicated by an arrow placed on the branch, and the multiplication factor (transmittance or transfer function) is indicated by a letter placed near the arrow.

To make a comparison, the signal flow graph of conventional Go-Back-N protocol is first shown in Figure 4.1. In the figure, $R(i)$ is used to represent the situation that the ith packet has just been transmitted or retransmitted while $D(i)$ the situation that ACK/NAK is expected in the sender. p is the probability that error is occurred in a packet, i.e., packet error rate. It is assumed that any error would be detected. $q = 1 - p$ is the probability that packet is transmitted error-free.

Figure 4.1 Signal flow graph of Go-Back-N protocol

z is the time to transmit one packet and assuming that in one round-trip delay, s packets are transmitted. This is denoted as z^s in the signal flow graph.

Note that the reverse channel, i.e., the channel sending acknowledgment back, is considered error-free because of following two reasons. 1) ACK/NAKs are usually small so the probability that they are corrupted is hence small; 2) Cumulative acknowledgment allows an ACK acknowledge all packets already received [38].

The signal flow graph of Go-Back-(N, M) protocol is shown in Figure 4.2. Note that once error is detected in packet i, retransmission begins from packet $i - M$

Figure 4.2 Signal flow graph of Go-Back-(N, M) protocol

at node $R(i - M)$ for Go-Back-(N, M), while retransmission begins just from packet i at node $R(i)$ for Go-Back-N in Figure 4.1. For any packet, e.g., packet i, in addition to node $D(i)$, there are another M nodes, $i_1, i_2, \cdots, i_M$. Signal flow arrives

at i_j $(1 \leq j \leq M)$ when error is detected at $D(i + M + 1 - j)$ and retransmission begins from packet $i + 1 - j$. For example, if $M = 3$ and error is detected in packet 7, retransmission will begin from packet 4 and go through the node 4_1, 5_2, 6_3 and finally reach $D(7)$ to be checked again. Note that these M nodes, i_1 to i_M, are different from each other because packet i is retransmitted when error is found in any of the packet with number from i to $i + M$. Node $D(i)$ and i_M to i_1 represent the packet i when error occurs in packet i and packet $i + 1$ to $i + M$, respectively.

Since all the retransmission flows are similar, one flow is analyzed, e.g., packets are retransmitted and checked at $(i - M)_1$, $(i - M + 1)_2$ to $D(i)$. Let $H(z)$ be the transfer function of transmitting two continuous packets, e.g., packet $i - 1$ and packet i. Repeatedly applying the serial and parallel merge to simplify the signal flow graph in Figure 4.2 gives

$$H(z) = \frac{qz \left(1 - qz - pz^{s+1} + p\,q^M\, z^{s+M+1}\right)}{1 - qz - pz^{s+1} + p\,q^{M+1}\, z^{s+M+2}}. \tag{4.1}$$

If transmitting L packets, the transfer function for sending all these packets is

$$H_L(z) = H(z)^L = \left[\frac{qz \left(1 - qz - pz^{s+1} + p\,q^M\, z^{s+M+1}\right)}{1 - qz - pz^{s+1} + p\,q^{M+1}\, z^{s+M+2}}\right]^L. \tag{4.2}$$

Physically, $\left.\frac{d\,H_L(z)}{dz}\right|_{z=1}$ represents the average time taking to traverse L packets in signal flow graph [37] and it is

$$\left.\frac{d\,H_L(z)}{dz}\right|_{z=1} = \frac{(1 + ps)\,L}{q^{M+1}}. \tag{4.3}$$

Therefore, the throughput of the Go-Back-(N, M) protocol η_{gbnm} is obtained through the inverse of $\left.\frac{d\,H_L(z)}{dz}\right|_{z=1}$ with $L \to \infty$,

$$\eta_{\text{gbnm}} = \lim_{L \to \infty} \frac{L}{\left.\frac{d\,H_L(z)}{dz}\right|_{z=1}} = \frac{q^{M+1}}{1 + ps}. \tag{4.4}$$

Note that the first M and last M packets are not considered in above derivation, whose signal flow graphs are different from above. But same result can be obtained

when L goes to infinity. One can see η_{gbnm} changes with q to the order of $M + 1$. If q is big, e.g., $q \approx 1$, the impact of retransmission of M more packets is small. If q is small, η_{gbnm} drops quickly. Luckily, M is small in most applications. Note that when $M = 0$, the throughput becomes $\frac{q}{1+ps}$, which is the throughput of conventional Go-Back-N protocol [39].

4.2 Optimal Case for Go-Back-(N, M) Protocol

Go-Back-(N, M) protocol always retransmits M more packets to correct possibly long-propagated errors. Eq.(4.4) shows that its throughput changes with q^{M+1}. When q is small, even a small M makes the throughput drop quickly. This can be improved if the location of error is known and only the packet that contains the error is retransmitted.

For a packet with length L and an error propagation distribution with PDF $f(x)$ and CDF $F(x)$, the probability that an error found in the packet does exist in the packet is

$$\Psi(F, L) = \frac{1}{L} \int_0^L F(x)\, dx. \tag{4.5}$$

Then the probability that an error found in the packet but actually exist in previous packet, i.e., error propagates through 1 packet, is $\Psi(F, 2L) - \Psi(F, L)$, and more generally, the probability that the error propagates through i packets, $0 \le i \le M$, is $\Psi[F, (i + 1)L] - \Psi(F, iL)$. If retransmission starts from packet i, the corresponding throughput is $\frac{q^{i+1}}{1+ps}$, and overall throughput for this optimal case is

$$\eta_{\text{gbnm\_best}} = \sum_{i=0}^{M} \frac{q^{i+1}}{1 + ps} \left\{ \Psi[F, (i + 1)L] - \Psi(F, iL) \right\}. \tag{4.6}$$

However, in practice the location of error is unknown and $\Psi(F, L)$ generally cannot determine the retransmission position. For a good error propagation distance PDF, such as in the text transmission, the error location can be determined with

a high probability. To do this, a propagation distance l_{full} is calculated such that $F(l_{\text{full}})$ almost approaches 1. For a packet with length $L > l_{\text{full}}$, if error is found at the position after l_{full} bits, the error is located in this packet with a high confidence and retransmission just starts from it. If error is found within l_{full} bits, previous packet is retransmitted. The throughput for this case (not as good as the optimal case but much more practical) is

$$\eta_{\text{gbnm\_better}} = \frac{L - l_{\text{full}}}{L}\frac{q}{1 + ps} + \frac{l_{\text{full}}}{L}\frac{q^2}{1 + ps}, \tag{4.7}$$

where the probability that the error traverses more than 1 packet is ignored because $F(l_{\text{full}}) \approx 1$. Generally, the smaller l_{full}, the better performance obtained.

4.3 Throughput of Go-Back-(N, M) Protocol with Packet Combining

As explained in Section 3.2, packet combining can be performed on the retransmitted packets since the delay PDF is not uniformly distributed. Two cases are considered. In first case, packet combining is performed only on the packet that is being detected and retransmitted, i.e., only 1 packet is buffered. In second case, all the N packets after the packet in first case are buffered and packet combining is performed on all these packets, just as shown in Figure 3.3.

For the first case, to simplify the derivation, it assumes that by using packet combining, the overall packet error rate is reduced by the ratio of α, where $0 < \alpha < 1$. Denoting the new packet error rate as $P = \alpha p$, the probability that packet is correct is $Q = 1 - P$.

The signal flow graph of Go-Back-(N, M) protocol with packet combining is shown in Figure 4.3. To simplify, only the node from $i - M$ to $i + 1$ are shown.

Note that for each packet i, another node, $D'(i)$, is added, which is different from $D(i)$ because packet combining is performed at $D'(i)$, while there is no retrans-

Figure 4.3 Signal flow graph of Go-Back-(N, M) protocol with packet combining

mitted packet at node $D(i)$. Packet combining is performed at node $(i - M)_1$, $(i - M + 1)_2, \cdots, (i - 1)_M$ and $D'(i)$.

The transfer function for transmitting L packets can be obtained as

$$
\begin{aligned}
H_L(z) &= H(z)^L \\
&= \left(\frac{qz - Qqz^2 - Pqz^{s+2} + PqQ^{M+1}z^{s+M+3} + pQ^{M+1}z^{s+M+2} - pQ^{M+2}z^{s+M+3}}{1 - Qz - Pz^{s+1} + PQ^{M+1}z^{s+M+2}} \right)^L.
\end{aligned}
$$

(4.8)

After calculating $\left. \frac{dH_L(z)}{dz} \right|_{z=1}$, finally the throughput is obtained as

$$
\eta_{\text{comb}} = \frac{Q^{M+1}}{ps + \frac{p}{P}(1 - Q^{M+2}) + qQ^{M+1}}.
$$

(4.9)

Since $P = \alpha p$, the throughput can be re-written as

$$
\eta_{\text{comb}} = \frac{(1 - \alpha p)^{M+1}}{ps + [1 - (1 - \alpha p)^{M+2}]/\alpha + q(1 - \alpha p)^{M+1}}.
$$

(4.10)

For given p, s, and M, η_{comb} changes with α and their relation is shown in Figure 4.4. Figure 4.4 shows that η_{comb} increases rapidly when α is big ($\frac{1}{\alpha}$ is small), e.g., $\alpha < 1$. When $\frac{1}{\alpha}$ is large, (around 5 in Figure 4.4), η_{comb} almost approaches its

Figure 4.4 Relation between η_{comb} and α, for given p, s and M.

maximum value. This means one can simply apply the maximum throughput that the packet combining can achieve. η_{comb} will obtain its maximum value when $\frac{1}{\alpha}$ goes to infinity, which is

$$\eta_{\text{comb\_max}} = \frac{1}{ps + (M+2)p + q}. \tag{4.11}$$

To see how much throughput gain can packet combining obtain, the gain is calculated,

$$
\begin{aligned}
G &= \frac{\eta_{\text{comb\_max}}}{\eta_{\text{gbn}}} \\
&= \frac{1 + ps}{1 - (m + s + 1)p^2 + (m + s)p}. \tag{4.12}
\end{aligned}
$$

Figure 4.5 shows the value of G with respective to p, $0 \le p < 1$. There are two points with $G = 1$. When $p = 0$, both scheme obtain 100% of the throughput. When $p < \frac{M}{s+M+1}$, $G < 1$. This means the detriment of retransmitting M more packets is bigger than the merit of packet combining, and at $p = \frac{\sqrt{(s+1)(M+1)(s+M+1)} - (s+M+1)}{s^2 + Ms + s}$, G gets its minimum value. When $p > \frac{M}{s+M+1}$, packet combining outperforms the redundancy of retransmitting M more packets and $G > 1$ is obtained.
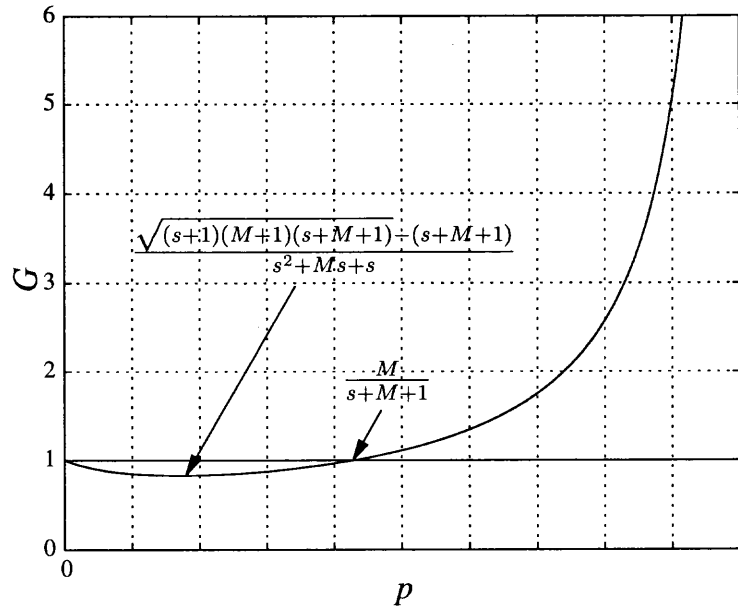
Figure 4.5 Packet combining gain

For the second case, N more packets are buffered. Since packet combining is performed to all these packets, the packet error rate is reduced by approximately $\frac{\alpha}{N}$. The result in Eq.(4.10) is used and it gives

$$\eta_{\text{comb\_N}} = \frac{(1 - p\alpha/N)^{M+1}}{ps + N/\alpha\,[1 - (1 - p\alpha/N)^{M+2}] + q(1 - p\alpha/N)^{M+1}}. \tag{4.13}$$

The throughput is bigger than that in the first case, and it increases with N, which is shown in the simulation.

4.4 Simulation Results

4.4.1 Selection of Code Rate for JARQ and Conventional ARQ

For the conventional ARQ schemes, the selected code rate, $\frac{k}{n}$, must be small enough so that the probability of catastrophic error (undetected error pattern) is very low. Although with JARQ protocol, a channel error will be detected eventually, to draw a fair comparison, $P_E\,P_{MIS}$, the probability of undetected error in JARQ, is equated to the probability of catastrophic error in conventional ARQ systems. The difference between the two scenarios should be emphasized. With conventional ARQ protocols,

when the channel decoder supplies an incorrect codeword to the source decoder, there is no way to recover from this error. While with JARQ, a missed error will always propagate and garble the remaining data and eventually, it will be detected.

For plain English text files, $P_{mis} \approx 0.0268$ [16]. Since the compression ratio $R \approx 1.47$ is small, $P_{MIS}(l) \approx 0.0268^l$. In the simulation performed here, ATM cells is used as the transmitted packet, where the packet size is 53 bytes [40]. For a marked block size of $m = 30$ and $R = 1.47$, the number of marked blocks in an ATM cell is $l = \frac{53R}{m}$. The code rate is chosen to bound the misdetection probability by 10^{-11}, i.e.,

$$P_{MIS}(l) = P_{mis}^{(\frac{1}{2}+M)\,53R/m} \approx 0.0268^{(\frac{1}{2}+M)\,53R/m} < 10^{-11}. \tag{4.14}$$

This gives $M = 2$ for the above parameters.

For image data, since the above approximation cannot be used, simulation is relied on to find an m that bounds us to the same bound of misdetection probability. If applying Go-Back-(N, M) with $M = 2$, the value of m is found to be around 20 from simulation. Thus the code rates are $\frac{30}{31}$ and $\frac{20}{21}$ for text and image transmission respectively.

The code rate of conventional Go-Back-N protocols, $\frac{k}{n}$, is about to determined to give a probability of catastrophic error in the same vicinity for the same packet size. Eq.(4.15), from [29], can provide a bound for this probability using linear block codes (e.g., CRC),

$$P_{\text{undetected}} \leq 2^{-(n-k)}[1 - (1 - p_b)^n]. \tag{4.15}$$

Thus, for a given n, after setting $P_{\text{undetected}} \approx 2^{-(n-k)}\,[1 - (1 - p_b)^n] = P_E\,P_{MIS}$, one can solve for k and obtain the values of the code rate, $\frac{k}{n}$, with ARQ. A codeword length n equal to the packet length as the entire ATM cell is used i.e., $n = L = 53 \times 8$ bits. This gives $n - k \approx 37$ bits and $\frac{k}{n} \approx 0.9127$ for conventional ARQ.

4.4.2 Throughput Comparison

Simulation is carried out using adaptive arithmetic coding [25]. Plain English text and the 256×256 LENA in the DCT domain are used.

Figure 4.6 shows the simulation results obtained for throughput versus BER, using $N = 4$ and $M = 2$. Figure 4.7 repeats the same simulation for the case of $N = 64$ and $M = 2$. The figures show that JARQ obtains a larger throughput than ARQ at low BER's because of its higher code rate, for either text or image transmission. Notice that as the BER increases, the performance of JARQ degrades more than with conventional ARQ (crosses over in the figure). This is because at a high BER, the detriment of the extra packet transmission is more than the gain obtained from increasing the code rate.
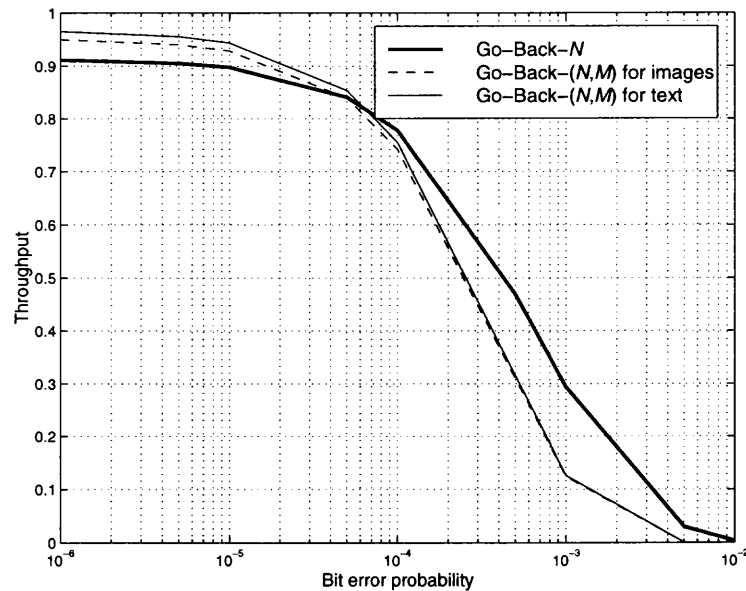
Figure 4.6 Throughput comparison of Go-Back-(N, M) and Go-Back-N protocols ($N = 4$ and $M = 2$)

Figure 4.8 and Figure 4.9 show the performance of Go-Back-(N, M) with packet combining for $N = 4$, $M = 2$, and $N = 64$, $M = 2$, respectively. Text transmission is used in these figures (similar results are obtained for image transmission). Overall, JARQ with packet combining improves throughput performance, especially at high
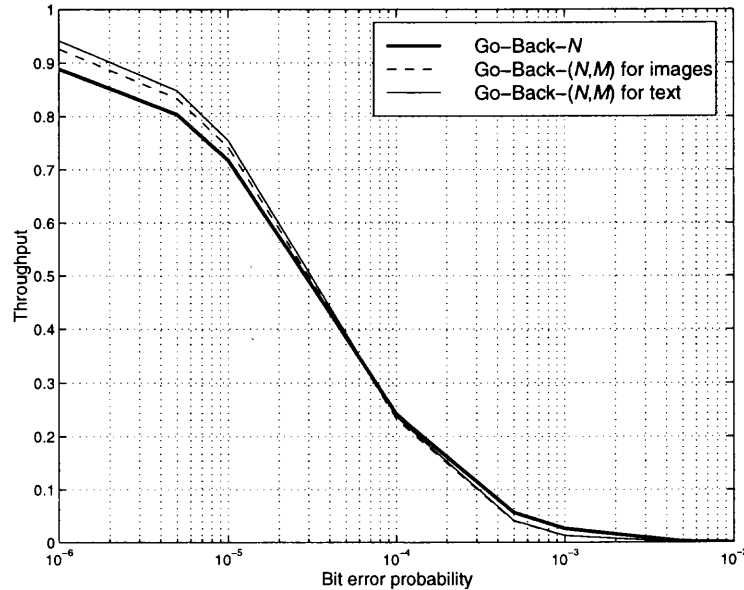
Figure 4.7 Throughput comparison of Go-Back-(N, M) and Go-Back-N protocols $(N = 64$ and $M = 2)$

BER's. Notice that packet combining gives more throughput gain for a large window size than for a small one. This should be expected since two copies of a long frame with errors are more likely to contain non-overlapping error.

4.5 Summary

In this chapter, the throughput of JARQ protocol is analyzed for independent channel by using signal flow graph. Suffered from the delayed detection, the throughput changes to the order of number of extra retransmissions. However, this impact is alleviated when BER is small. At high BER's, packet combining is introduced and significant throughput gain is achieved. In addition, The throughput is increased with a larger code rate, compared with conventional ARQ scheme. The simulation results validate the analysis.

Figure 4.8 Throughput of Go-Back-(N, M) protocol using packet combining ($N = 4$ and $M = 2$)

Figure 4.9 Throughput of Go-Back-(N, M) protocol using packet combining ($N = 64$ and $M = 2$)

CHAPTER 5

THROUGHPUT ANALYSIS OF JARQ PROTOCOL ON NONINDEPENDENT CHANNEL

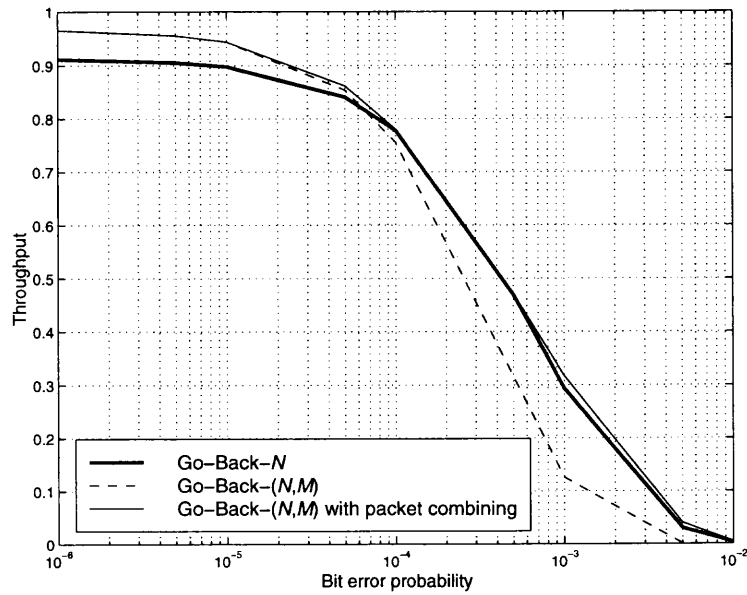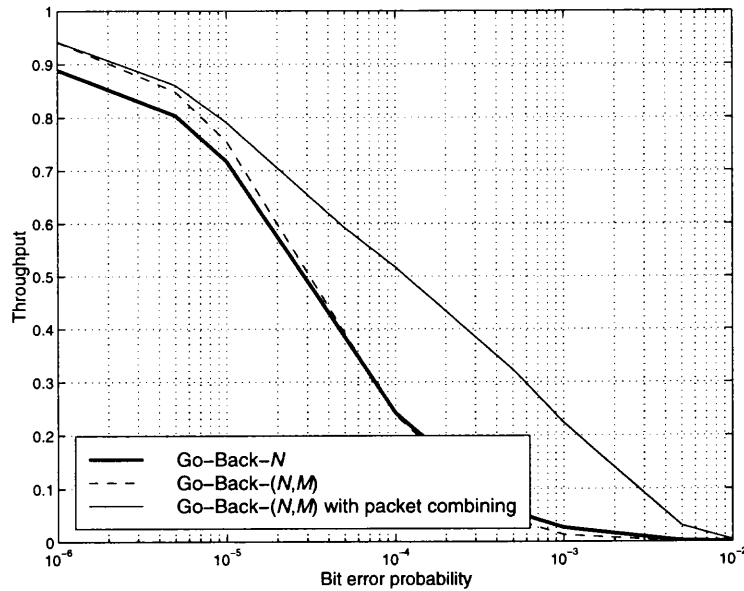Chapter 3 proposes a JARQ protocol for the joint lossless-source and channel coding scheme introduced in Chapter 2. The throughput of this protocol on independent channel is analyzed in Chapter 4. In this chapter, its throughput on nonindependent channel is analyzed.

5.1   Introduction

Unlike the independent channel which is modeled by bit error rate (BER), a nonindependent channel is often modeled by Markov process. Gilbert [41] first studied the Markovian type of channel errors with two-state model. Later Fritchman [42] proposed finite-order model which can be represented by a finite-order Markov process. The kth-order Markovian channel model applies a k-dimensional transition matrix to represent the relation between the correctness of a received packet and the error conditions of its k preceding packets. A gap error model was also proposed to simulate nonindependent channel by Kanal and Sastry [43] which models the number of correct (erroneous) packets between two consecutive erroneous (correct) packets as random variables.

Although the second or higher-order Markov process provides a more accurate model of nonindependent channel condition, recent studies by Wang and Chang [44], Abdi [45], and Zorzi *et al.* [46] show that a first-order Markovian channel which uses only the information of immediately preceding packet is adequate to model the nonindependent channel. The amount of uncertainty in the current packet provided by the packets preceding the previous one is negligible.

In the rest of this chapter, Section 5.2 describes the first-order Markovian channel model. The throughput of Go-Back-(N, M) protocol under nonindependent

channel is analyzed in Section 5.3. The performance of JARQ protocol without packet combining and JARQ protocol with packet combining are simulated in Section 5.4.1 and Section 5.4.2, respectively. Final section draws some conclusions.

5.2 Nonindependent Channel Model

The two-state models by Gilbert [41] and Elliot [47] are examples of first-order Markov process. It consists of two states which are called G (for good) and B (for bad or for burst). Similar ON-OFF model is also widely used, where an ON (active) state and an OFF (silent) state are introduced [48–50]. Transitions are made between two states according to transition probabilities. Burst errors are generated bit by bit each time the B (or ON) state has arrived. A Similar threshold model is proposed by Zorzi *et al.* [51] who extended the model to generate error frame by frame, or packet by packet.

The nonindependent channel model used in this chapter is based on the threshold model in [51] and summarized in [52]. It is shown that a sequence of packet is correct or erroneous can be approximated by means of a simple two-state Markov chain whose transition probability matrix is given by

$$M_F = \begin{bmatrix} q & 1-q \\ 1-p & p \end{bmatrix}, \tag{5.1}$$

where q and $1-p$ are the probabilities that the jth packet is correct, given that the $(j-1)^{\text{th}}$ packet was correct or incorrect, respectively. p and $1-q$ are the probabilities that the jth packet is incorrect, given that the $(j-1)^{\text{th}}$ packet was incorrect or correct, respectively. Note that $\frac{1}{1-p}$ represents the average length of a burst of packet errors. The channel condition of forward channel (i.e., sender sends packet to receiver) is focused and the transition matrix of backward channel (i.e., receiver responds acknowledgment to sender), M_B, is considered error-free. (See Section 4.1.) The error pattern relation between two packets being x packets apart

is

$$M_F(x) = (M_F)^x = \begin{bmatrix} q(x) & 1-q(x) \\ 1-p(x) & p(x) \end{bmatrix}.$$ (5.2)

The steady state can be obtained when $(M_F)^x$ approaches a matrix A with $x \to \infty$. Each row of A is the same probability vector $\alpha = [\pi_c \quad \pi_e]$, where π_c and π_e are the steady state probability of a correct transmission or an incorrect transmission, respectively [53]. Also from [53], the steady state probability is,

$$\alpha = [\pi_c \quad \pi_e] = \begin{bmatrix} \dfrac{1-p}{2-p-q} & \dfrac{1-q}{2-p-q} \end{bmatrix}.$$ (5.3)

For a fading multipath channel with a fading margin F, the average frame error rate (FER), i.e., packet error rate, can be found in [54] as

$$P_E = 1 - e^{-1/F}.$$ (5.4)

From [51], p is given by

$$p = 1 - \frac{Q[\theta, J_0(2\pi f_d T)\theta] - Q[J_0(2\pi f_d T)\theta, \theta]}{e^{1/F} - 1},$$ (5.5)

where

$$\theta = \sqrt{\frac{2}{F[1 - J_0^2(2\pi f_d T)]}}.$$ (5.6)

In the above, $J_0(\cdot)$ is the Bessel function of the first kind and zeroth order. $f_d T$ is the normalized Doppler bandwidth which describes the correlativity or burstness in the nonindependent channel. $Q(\cdot, \cdot)$ is the Marcum Q function, given by

$$Q(x, y) = \int_y^\infty e^{-\frac{x^2 + w^2}{2}} I_0(xw) \, w \, dw,$$ (5.7)

where I_0 is the modified Bessel function of the first kind and zeroth order. Given F and $f_d T$, the Markov parameter p and q are obtained from Eq.(5.4) to Eq.(5.7).

5.3 Signal Flow Graph of Go-Back-(N, M) Protocol and Throughput Analysis

The performance of ARQ protocol on nonindependent channel has been widely studied [55–58]. Cho and Un [55] investigated the effect of forward/backward channel memory on two modified Go-Back-N protocols. Lu and Chang [56] used k^{th}-order Markovian channel model and gap error model [43]. The performance of Go-Back-N protocol with unreliable feedback and the comparison of Go-Back-N and selective repeat protocols on nonindependent channel were analyzed by Zorzi and Rao [57] and Chuang [58], respectively. In this study, the first-order Markovian channel model is used and performance of the delayed detection, i.e., M more retransmitted packets, is investigated [59–61].

If transmitting L packets, the signal flow graph of the Go-Back-(N, M) protocol under nonindependent channel is shown in Figure 5.1. Similar notations to that
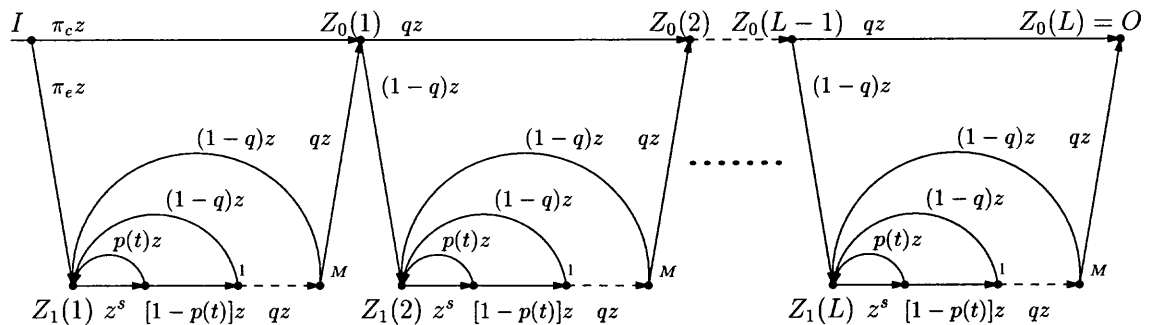
Figure 5.1 Signal flow graph of Go-Back-(N, M) protocol on nonindependent channel

in [55] are used. Node I and node O denote input and output nodes, respectively. Any path leading from I to O corresponds to a successful transmission of these L packets. z is the time to transmit one packet and assuming that in one round-trip delay, s packet are transmitted. This is denoted as z^s in signal flow graph. Node $Z_0(i)$ and node $Z_1(i)$, $1 \leq i \leq L$, denote the ith packet is transmitted correctly or incorrectly, respectively.

Starting from node I, packet is either transmitted correctly with probability π_c to node $Z_0(1)$, or transmitted incorrectly with probability π_e to node $Z_1(1)$. At node $Z_1(1)$, retransmission is requested. After time $t = s + 1$, i.e., round-trip delay plus the time to transmit one packet, the retransmitted packet is either incorrectly received with probability $p(t)$, the probability that current packet is erroneous if the $(s+1)^{\text{th}}$ preceding packet is erroneous, or correctly received with probability $1 - p(t)$, the probability that current packet is correct if the $(s + 1)^{\text{th}}$ preceding packet is erroneous. Since M more packets have to be retransmitted and if the first one is retransmitted correctly, the next packet is either incorrectly received and status is back to $Z_1(1)$ with probability $1 - q$, the probability that current packet is erroneous if the immediately preceding packet is correct, or correctly received with probability q, the probability that current packet is correct if the immediately preceding packet is correct, as well.

After M consecutively successful retransmission, one packet is released and detection process arrives at node $Z_0(1)$. At $Z_0(1)$, packet is either transmitted correctly with probability q to node $Z_0(2)$, or transmitted incorrectly with probability $1 - q$ to node $Z_1(2)$, since the previous packet is correctly received. After that, signal flow repeats as the above.

Let $H(z)$ be the transfer function of transmitting these L packets. Note that the signal flow graph consists of two similar flows with minor difference. The transition starting from node I has probability π_c and π_e, while the transition starting from node $Z_0(i)$, $1 \le i < L$, has probability q and $1 - q$. The transfer function from node I to node $Z_0(1)$ is obtained first by applying the serial and parallel merge in signal flow graph. Let $t = s + 1$, round-trip time plus the time to transmit a packet, which is the time from the start of transmission of a packet to the receipt of its acknowledgment,

the transfer function is

$$H_{L=1}(z) = \pi_c z + \frac{\pi_e z[1-p(t)]z^t q^M z^M (1-qz)}{1-qz-p(t)z^t(1-qz)-[1-p(t)](1-q)z^{t+1}(1-q^M z^M)}. \quad (5.8)$$

The transfer function between node $Z_0(i)$ and node $Z_0(i+1)$, $1 \leq i < L$, can be obtained, by replacing π_c with q and π_e with $1-q$ in Eq.(5.8), as

$$H_{1 \leq i < L}(z) = qz + \frac{(1-q)z[1-p(t)]z^t q^M z^M (1-qz)}{1-qz-p(t)z^t(1-qz)-[1-p(t)](1-q)z^{t+1}(1-q^M z^M)}. \quad (5.9)$$

Finally the transfer function of transmitting L packets is obtained as

$$H_{L>1}(z) = H_{L=1}(z)[H_{1 \leq i < L}(z)]^{L-1}$$
$$= H_{L=1}(z)\left\{qz + \frac{(1-q)z[1-p(t)]z^t q^M z^M (1-qz)}{1-qz-p(t)z^t(1-qz)-[1-p(t)](1-q)z^{t+1}(1-q^M z^M)}\right\}^{L-1}. \quad (5.10)$$

Since $\left.\frac{d\,H_L(z)}{dz}\right|_{z=1}$ represents the average time taking to traverse L packets in the signal flow graph [37], the throughput can be obtained by limiting L to infinity as

$$\eta = \lim_{L \to \infty} \frac{L}{\left.\frac{d\,H_L(z)}{dz}\right|_{z=1}}. \quad (5.11)$$

Therefore, the throughput when $L = 1$ is

$$\eta_{L=1} =$$
$$\left\{\pi_c + \pi_e \frac{q+p(t)t-qp(t)(t+1)+(1-q)[1-p(t)](t+1)-[1-p(t)]q^{M+1}}{q^M(1-q)[1-p(t)]}\right\}^{-1}. \quad (5.12)$$

and the throughput when L approaches infinity,

$$\eta_{L \to \infty} = \frac{q^M[1-p(t)]}{q+p(t)t-qp(t)(t+1)+(1-q)[1-p(t)](t+1)}. \quad (5.13)$$

5.4   Simulation Results

5.4.1   Simulation Results without Packet Combining

In the simulation, the threshold model previously described is used. Choosing different values of fading margin (F) and normalized Doppler bandwidth $(f_d T)$,

different Markov parameter p and q are calculated and used in the simulation. With $f_d T = 0.01$, the channel is very correlated (long bursts of packet errors). With $f_d T = 1.0$, the channel becomes almost independent (short bursts of packet errors). The average packet error rate P_E is calculated by Eq.(5.4) and to make a comparison, the corresponding independent channel model is also considered with the same packet error rate. The round-trip delay is $s = 9$, i.e., $t = 10$. Go-Back-(N, M) protocol is used with $M = 2$.

Figure 5.2 shows the theoretical throughput calculated by Eq.(5.13) and the simulation results. $f_d T = 0.03$ and fading margin ranging from $F = 4.0$ dB to $F = 20.0$ dB are used. The throughput increases with fading margin. The figure shows the simulation results validate the analysis.
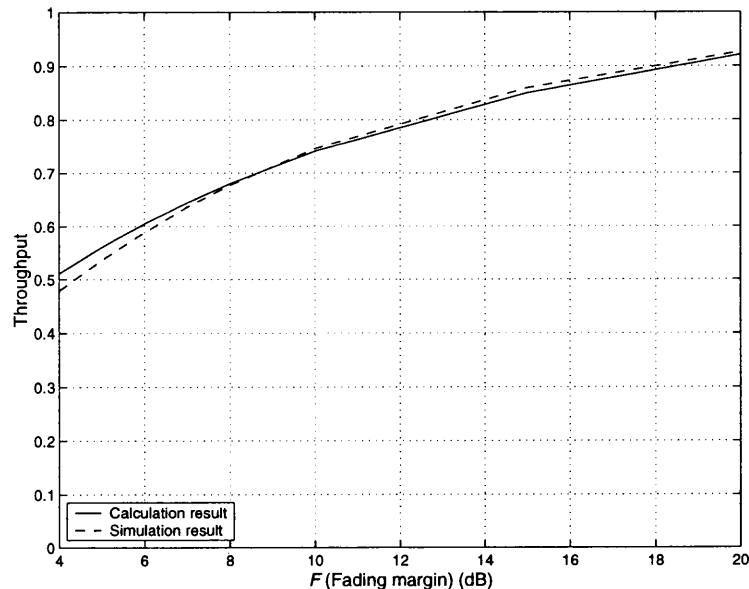
Figure 5.2 Comparison of theoretical throughput and simulation result of Go-Back-(N, M) protocol on nonindependent channel $(f_d T = 0.03)$

Figure 5.3 compares the throughput with different normalized Doppler bandwidth. $F = 5.0$ dB and $F = 15.0$ dB are used. The throughput of independent channel corresponding to the nonindependent channel with same P_E is also plotted to show the comparison. It is clear that the throughput increases (decreases)

when the channel becomes more correlated (independent). This means the transmission benefits from channel correlation. At around $f_dT \geq 0.3$, the channel can be considered almost independent as the throughput approaches that on the independent channel.
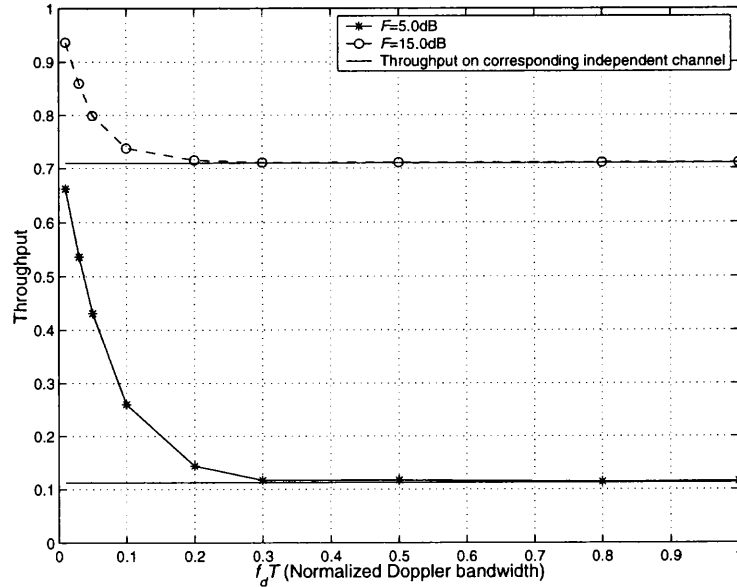
Figure 5.3 Throughput comparison of Go-Back-(N, M) protocol on nonindependent channel and independent channels ($F = 5.0$ dB and $F = 15.0$ dB)

5.4.2 Simulation Results with Packet Combining

Figure 5.4 to Figure 5.9 show the throughput of Go-Back-(N, M) on nonindependent channel with packet combining. The round-trip delay s is used as combining window size because it implies the number of packets which have performed packet combining in a round-trip delay time.

Figure 5.4 to Figure 5.7 compare the throughput with and without packet combining at different window size. The normalized Doppler bandwidths are $f_dT = 0.01, 0.03$, and 1.0 to represent different channel correlativity. One can see packet combining improves performance, especially at small F (large error rate) and large combining window size. At a large window size, e.g., $s = 64$ in Figure 5.7, the

performance on a less correlated channel (or almost independent channel for $f_d T = 1.0$) with packet combining is almost as good as that on a high correlated channel ($f_d T = 0.01$) without packet combining.

Figure 5.8 and Figure 5.9 show the throughput of packet combining using different combining window size with $F = 5.0$ dB and $F = 15.0$ dB, respectively. The channel is selected from a highly corrected case ($f_d T = 0.01$) to an almost independent case ($f_d T = 1.0$). The throughput on the corresponding independent channel is also shown as a comparison. The results validate the analysis by showing that the performance increases with the size of packet combining window and the correlativity of nonindependent channel.

Figure 5.4 Throughput comparison of Go-Back-(N, M) protocol on nonindependent channel with and without packet combining (combining window size $s = 4$. $f_d T = 0.01, 0.03,$ and 1.0)

Figure 5.5 Throughput comparison of Go-Back-(N, M) protocol on nonindependent channel with and without packet combining (combining window size $s = 10$. $f_d T = 0.01, 0.03$, and 1.0)

Figure 5.6 Throughput comparison of Go-Back-(N, M) protocol on nonindependent channel with and without packet combining (combining window size $s = 20$. $f_d T = 0.01, 0.03$, and 1.0)
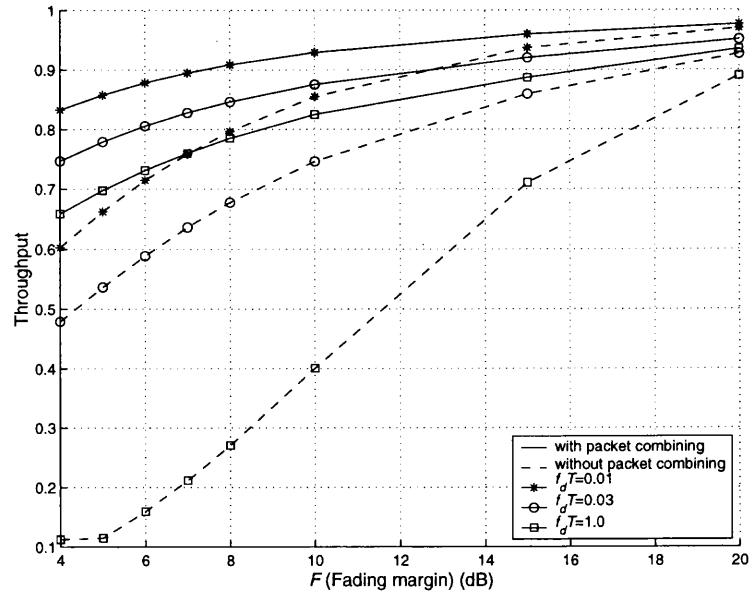
Figure 5.7 Throughput comparison of Go-Back-(N, M) protocol on nonindependent channel with and without packet combining (combining window size $s = 64$. $f_d T = 0.01, 0.03,$ and 1.0)
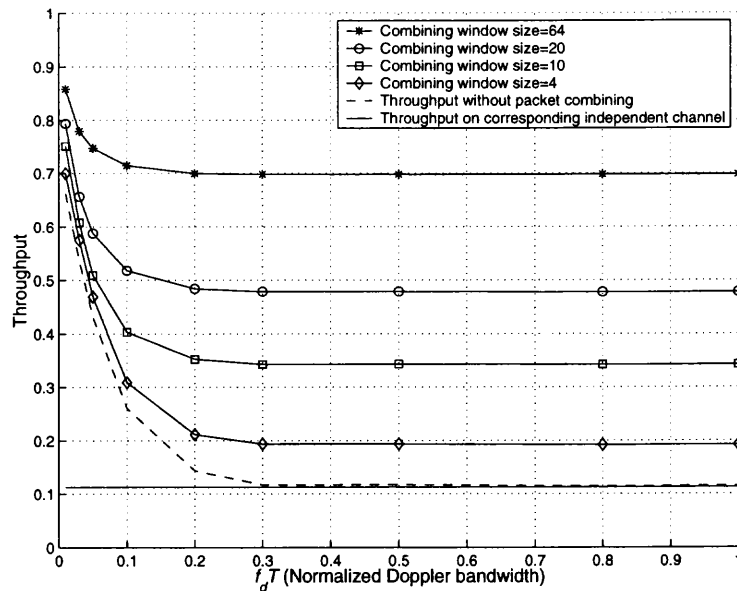
Figure 5.8 Throughput comparison of Go-Back-(N, M) protocol on nonindependent channel with and without packet combining (combining window size $s = 4, 10, 20,$ and 64. $F = 5.0$ dB)
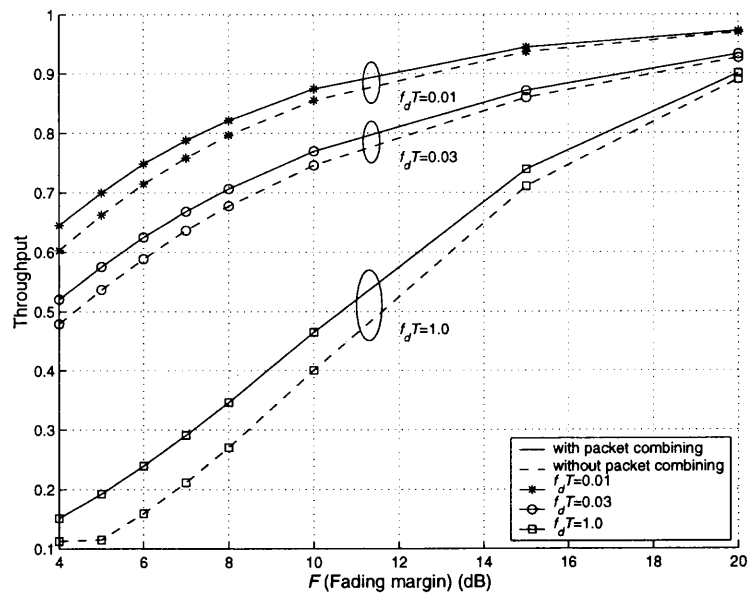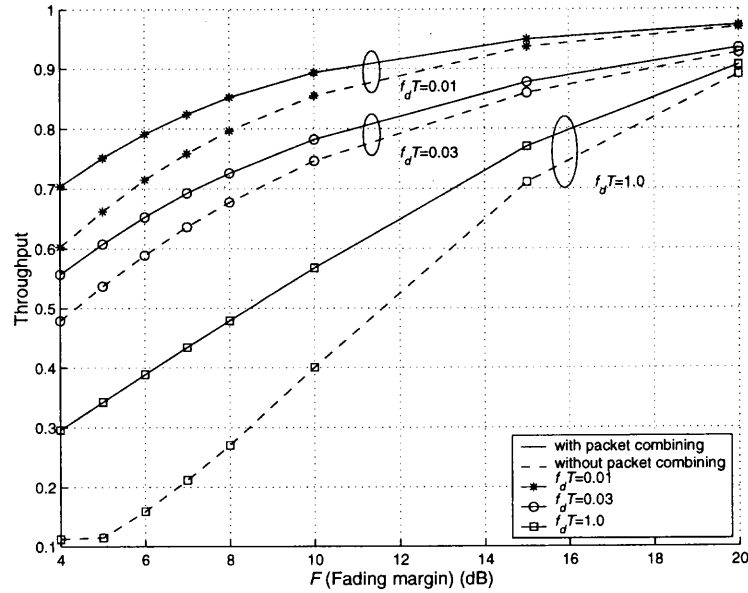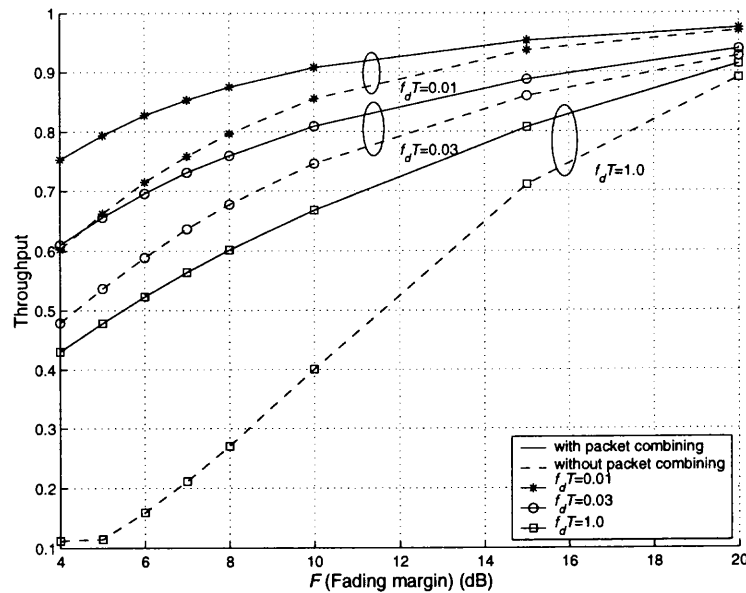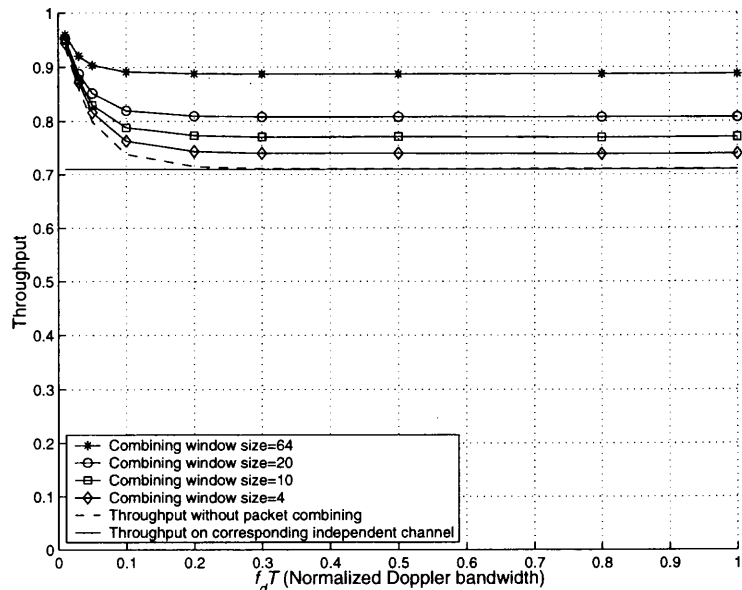
Figure 5.9 Throughput comparison of Go-Back-(N, M) protocol on nonindependent channel with and without packet combining (combining window size $s = 4$, 10, 20, and 64. $F = 15.0$ dB)

5.5 Conclusion

This chapter presents the performance of an ARQ protocol based on joint source and channel coding scheme on nonindependent channel. Simulation result shows it matches the theoretical throughput derived by signal flow graph. A good performance can be obtained at high correlation (at small f_dT). The throughput decreases when the channel becomes less correlated, i.e., more independent (at large f_dT), and approaches the throughput on the independent channel.

CHAPTER 6

JARQ APPLICATION TO WIRELESS TCP NETWORKS

One of an important application of joint source and channel coding is wireless communication where the limited channel source (bandwidth) requires an efficient system. This chapter applies JARQ protocol to wireless TCP networks to improve the performance of TCP on lossy wireless link. Several wireless TCP approaches are reviewed in Section 6.1. In Section 6.2, JARQ is introduced to the data link layer of wireless TCP networks as a radio link layer protocol. Section 6.3 compare the performance of TCP/ARQ and TCP/JARQ protocols and the simulation results show a significant performance improvement by error correction in data link layer with JARQ protocol.

6.1   Introduction

Due to the increasing need to share information between mobile users and to connect them to the Internet, wireless is becoming a popular way to connect mobile computers to provide applications like e-mail, web browsing, Telnet, mobile computing, etc. An efficient data transmission protocol should be applied to provide data exchange between mobile users in wireless networks and hosts in the existing Internet.

For the Internet, the most widely used transport layer protocol is Transmission Control Protocol (TCP) [62–64]. TCP provides a connection-oriented, reliable, end-to-end byte stream service by receiver's responding acknowledgment to transmitter, providing sliding window flow control, maintaining header and data checksum, and resequencing our-of-order data [62]. There are numerous rules regarding the initiation and termination of a TCP connection. Figure 6.1 shows the TCP connection by summarizing these rules in a state transition diagram.
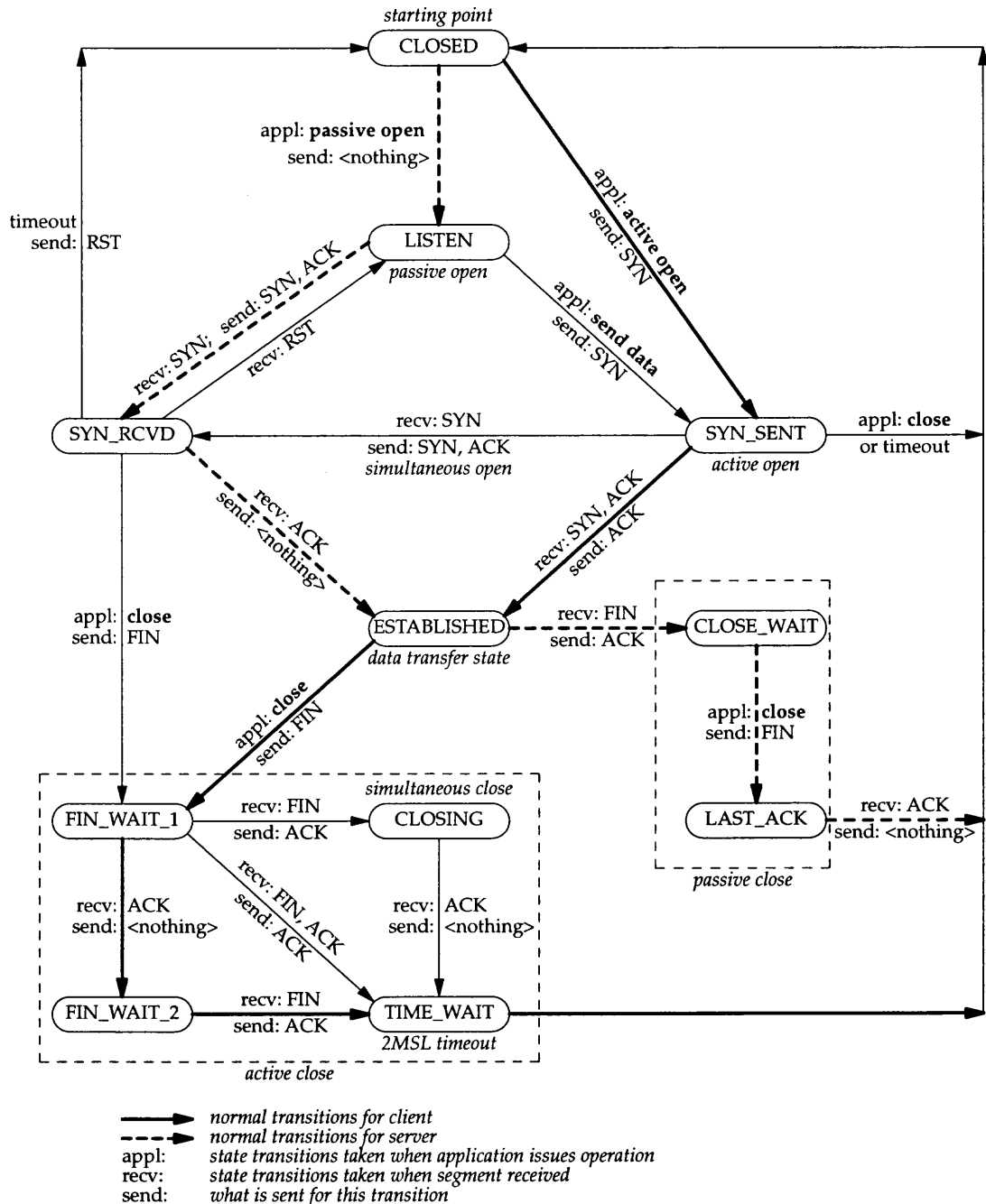
Figure 6.1 TCP state transition diagram. Reprinted from *TCP/IP Illustrated, Volume 1: The Protocols* by W. Richard Stevens. Copyright © 1994 by Addison-Wesley Publishing Company, Inc.

To provide an easy interaction between mobile users in wireless networks and hosts in the Internet, TCP should be applied to wireless networks to control data transmission, as well. However, TCP is designed to perform well in traditional wireless networks where the error rate is low and packet losses are mainly due to the congestion in the network. TCP responds to all packet losses by shrinking the congestion window size (*cwnd*) before retransmitting packets, and invoking congestion control and avoidance algorithm [65] or fast retransmit and fast recovery algorithm [66–68].

Although these algorithms work well to resolve congestion problems occurred in wireline networks, unfortunately they may fail in wireless networks. On lossy wireless link, the main reason for packet loss is the high error rate, not the congestion. Simply applying the congestion control and avoidance algorithm to wireless networks may result in an unnecessary reduction in the congestion window, hence in reduced throughput and degraded performance.

Recently, several approaches have been made to alleviate this problem and make the flow control scheme of TCP work efficiently in lossy wireless links. Balakrishnan *et al.* [69], Racherla *et al.* [70], and Wang and Tripathi [71] summarized and compared these approaches. The proposed TCP schemes for wireless networks can be classified in the following categories:

1. TCP/IP header compression. The 20-byte TCP header and 20-byte IP version 4 (IPv4) header can cause a significant amount of overhead in the application like Telnet, where a TCP segment may contain only 1 byte of data. With the combined 60-byte TCP/IP header in the new IP version 6 (IPv6), this overhead is more significant. It is observed that a large part of header does not change very much in a stream of packets, so the TCP/IP header can be compressed in such a way that the sender transmits a full header for the first time and transmits only the small changes for the successive packets. Jacobson [72]

proposed TCP/IP header compression for low-speed serial links and Degermark *et al.* [73] proposed the compression scheme on wireless networks. The recovery mechanism for original full header in case of error is also discussed.

2. Split-connection protocol. This protocol splits a TCP connection into two separate connections: one TCP connection between the sender and base station and the other between base station and receiver. One connection is on wireless link and the other is on wireline link for many mobile applications where the mobile user accesses hosts in the Internet. By splitting the TCP connection, the data flow over wireless link and data flow over wireline link are isolated from each other and the original TCP sender is shielded from the lossy wireless link.

   Indirect-TCP (I-TCP) [74] and mobile-TCP [75] are examples of this kind of protocol.

3. Snoop protocol. The snoop protocol introduces a "snoop agent" at base station which monitors the packets sent to and the acknowledgments sent back by the mobile user. A cache is maintained to buffer the unacknowledged packets and if a packet has been lost or corrupted, it will be retransmitted by the base station if the packet has been backed up in the buffer. The duplicated acknowledgments are suppressed and the sender is shielded from the packet loss. Balakrishnan *et al.* [76] proposed this kind of protocol.

4. Link layer solution. The idea is to add the error correction mechanism to lower layer, i.e., data link layer, and try to correct most of errors at this layer. The error that cannot be corrected by the limited attempts in data link layer will be finally forwarded to TCP layer. TCP layer will see the packet with much less error and congestion control and avoidance algorithm can work efficiently. There are lots of work in this area [52, 77–80].

The advantage of this approach is that TCP layer does not need modification and it works as usual since most of errors are corrected in lower layer and TCP layer is shielded from the error. A natural layered architecture is also maintained by this protocol.

5. Other methods includes explicit loss notification (ELN) [69] which explicitly tells the mobile users that whether the packet loss is due to congestion or channel error. Selective acknowledgment (SACK) [81] is also proposed which provides more information than the traditional cumulative acknowledgment to help suppress duplicate retransmissions and recover error.

Among the protocols introduced above, link layer solution is of interest because its protocol architecture allows us to introduce ARQ protocol in data link layer without modifying upper layers. A radio link protocol (RLP) is generally introduced and a TCP/RLP protocol stack is developed to reduce the error rate seen by the TCP layer and hence improve system performance. In particular, JARQ protocol is applied and the interaction between the data link layer with JARQ and TCP layer is analyzed to optimize the performance of TCP/JARQ protocol stack. The idea is natural because it shows in Chapter 1 that joint source and channel design may play an important role in wireless communication and the Internet to obtain good performance while meeting a satisfactory QoS.

6.2   TCP/RLP Protocol Stack

Due to the high link loss rate in wireless networks, to improve communication relia-bility and obtain good system performance, Section 6.1 shows that lower layer should provide a number of error control methods. A practical example is code division multiple access (CDMA) cellular system. In physical layer, forward error control (FEC) is implemented and specified in IS-95 [82]. In data link layer, RLP performing

a partial error recovery ARQ scheme is specified in IS-99 [83] and IS-707 [84] (an extended version of IS-99). This typical TCP/RLP implementation is shown in Figure 6.2.
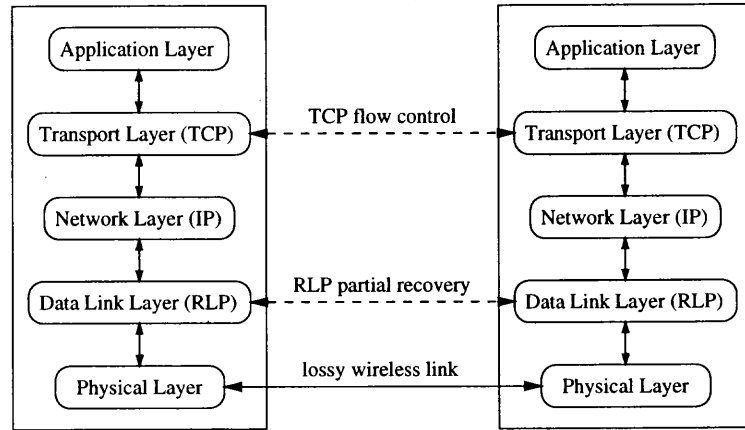
Figure 6.2 TCP/RLP protocol stack

In Figure 6.2, the data unit in RLP layer and TCP layer are called "segment" and "frame", respectively. If error occurs, RLP will first detect the error and perform a partial link error recovery through a limited number of frame retransmissions. It uses NAK-based ARQ protocol and will send back a NAK requesting retransmission of the lost frame in case of error. If the retransmitted frame is still erroneous, RLP will send back two NAKs and each NAK implies a retransmission of the requested frame. If these NAKs still cannot correct error, RLP will try the third attempt by sending back three NAKs. The number of attempts is limited and the default value is 3 in IS-99. After three unsuccessful retransmissions, RLP will abort the attempt and forward the error message to TCP layer. The congestion control and avoidance algorithm of TCP is the final resort to correct error.

When applying JARQ protocol as RLP, default values of maximum number of JARQ attempt (*retx_threshold*) and the newest frame number (*newest_frame_num*) are also maintained. If the frame number of incoming frame (*current_frame_num*) is smaller than *newest_frame_num*, the frame is discarded. Otherwise if the frame

is correct, it is sent to buffer and if a TCP segment is completely received with the frame, the TCP segment is forwarded to TCP layer. If the frame is erroneous, the number of retransmissions (num_retx) increases and if it is not larger than $retx\_threshold$, RLP will request retransmission. Otherwise the error message is passed to TCP layer and TCP layer will handle the error. The TCP/JARQ algorithm is shown by flow chart in Figure 6.3.
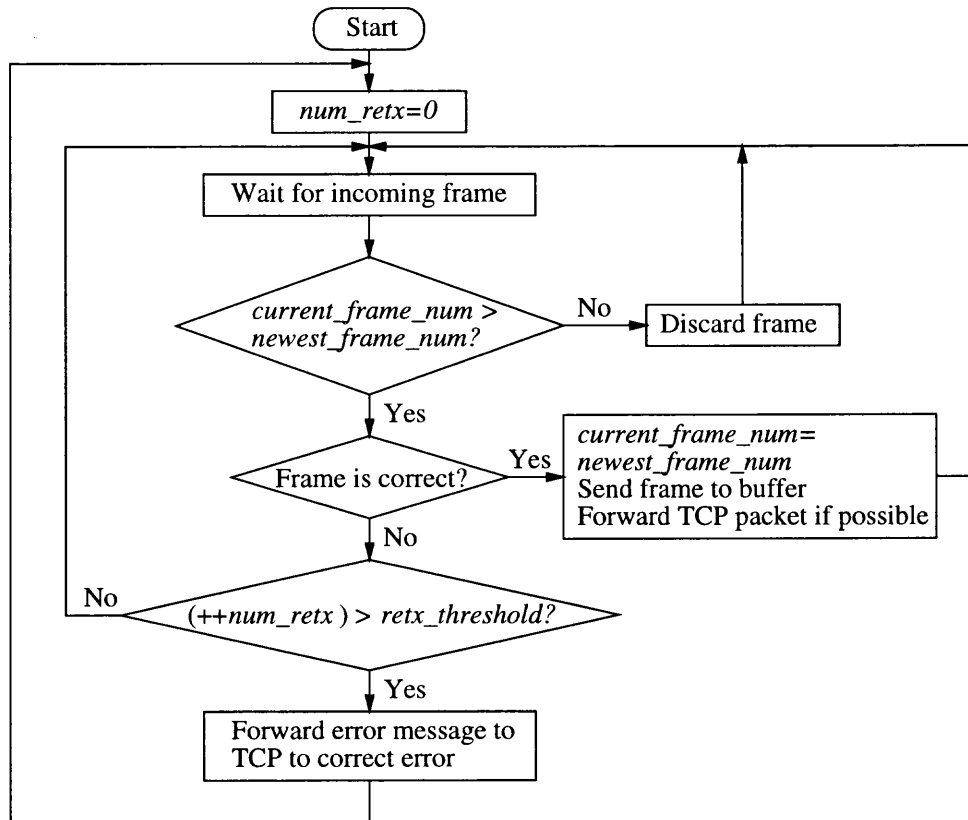
Figure 6.3 TCP/JARQ algorithm flow chart

6.3 Simulations

6.3.1 Simulation Tools

OPtimized Network Engineering Tool (OPNET) [85] is used as simulation tools. OPNET provides a comprehensive development environment supporting the modeling of communication networks and distributed systems. Both behavior and

performance of modeled systems can be analyzed by performing discrete event simulations. The simulation model is shown in Figure 6.4.
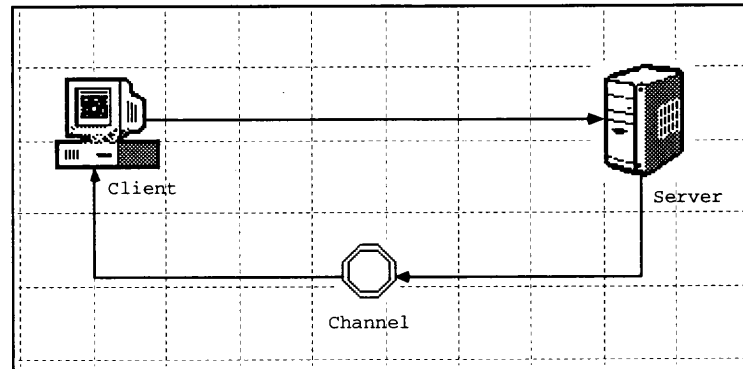
Figure 6.4 OPNET network model of TCP/RLP simulation

The model consists of two nodes representing client and server, respectively. JARQ protocol is implemented in the data link layer of client and server. An FTP session is opened by client to retrieve files from server. Server sends back data and a node representing lossy wireless channel is placed on the link from server to client. The Markovian threshold model [51] described in Chapter 5 is used as burst channel model. Traffic is monitored on the server side. The link from client to server is considered error-free because the traffic on the link is the acknowledgment sent from the client back to server. The acknowledgment packet is often small and since TCP uses cumulative acknowledgment, the link can be considered error-free. (See Section 4.1.)

Following parameters are selected in the simulation. Default TCP setting in OPNET is used with auto-assigned maximum transmission unit (MTU). Fast retransmission and fast recovery algorithm are enabled. Go-Back-(N, M) protocol with $M = 2$ is applied to RLP. The average number of data link layer frame contained in a TCP segment is 3. The retransmission threshold (i.e., maximum number of RLP attempts before error message is forwarded to TCP layer) uses following number: 0 (namely, RLP is not used), 1, 2, 5, and 10. For the nonindependent channel

model, normalized Doppler bandwidth is selected from 0.01, 0.03, 0.1, and 1.0 to represent different channel correlativity. Fading margin (F) is selected with corresponding average frame error rate ranging from 0 to 0.35. Other parameters of TCP protocol and channel model are not specified because the uniformed TCP throughput is analyzed and the system performance without using RLP is compared with that using RLP with different retransmission threshold.

6.3.2 Performance of TCP/JARQ Protocol Stack

Figure 6.5 to Figure 6.9 show the simulation results. TCP throughput versus different average frame error rate in system without using RLP is shown in Figure 6.5. TCP throughput increases as average frame error rate decreases. The most correlated channel ($f_dT = 0.01$) has the best performance and as the correlativity decreases, the performance approaches that on independent channel. This is the same result that is obtained in Chapter 5.

The advantages of using RLP with different retransmission threshold are shown in Figure 6.6 to Figure 6.8 with $f_dT = 0.01$, 0.1, and 1.0, respectively. The retransmission thresholds are 1, 2, 5, and 10. One can see RLP improves system performance significantly, and the larger retransmission threshold, the better performance. This means the persistence at RLP layer is beneficial to the system. Even with one retransmission attempt, the throughput can be almost doubled in most situations. However, as the attempt increases, e.g., from 5 to 10 in the figure, the throughput gain becomes less. Also as the correlativity decrease, the results approach that on independent channel. See Figure 6.8 and Figure 6.9.

Figure 6.10 and Figure 6.11 compare the TCP congestion control window size (*cwnd*) in system using RLP with one retransmission attempt and with 10 retransmission attempts to *cwnd* in system without using RLP, respectively. The results are obtained from above simulations and data are shown in a period of simulation time.
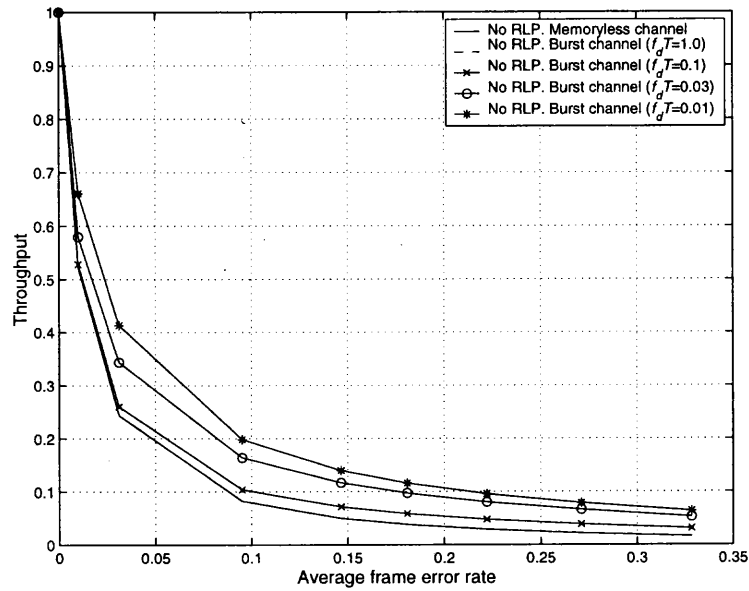
Figure 6.5 TCP throughput of system without RLP in data link layer

Figure 6.6 TCP throughput of system with RLP in data link layer (most correlated channel with $f_d T = 0.01$)
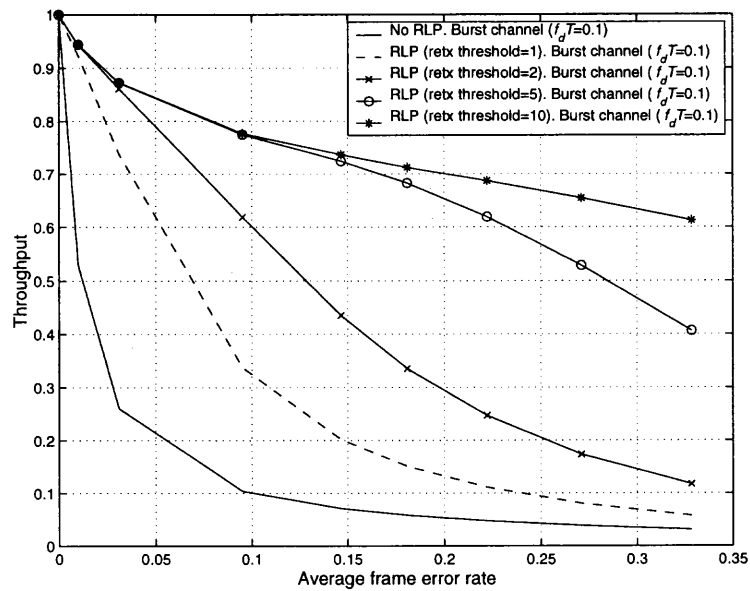
Figure 6.7 TCP throughput of system with RLP in data link layer (correlated channel with $f_d T = 0.1$)
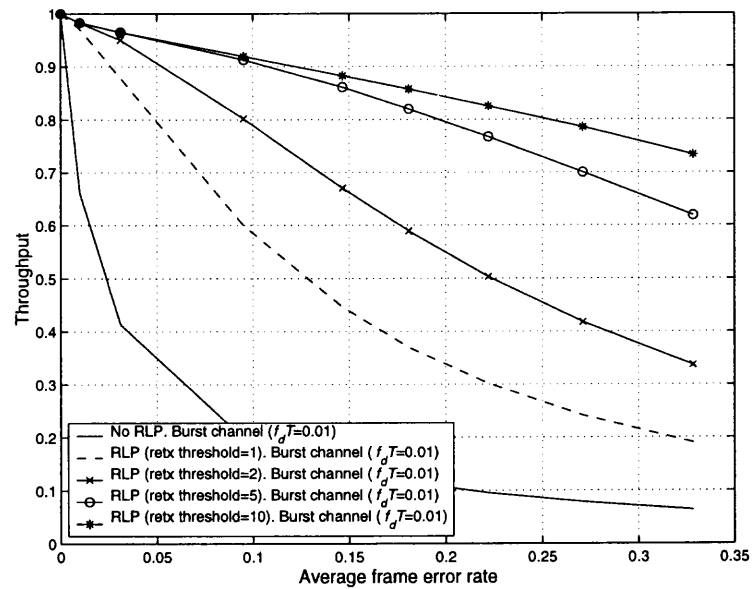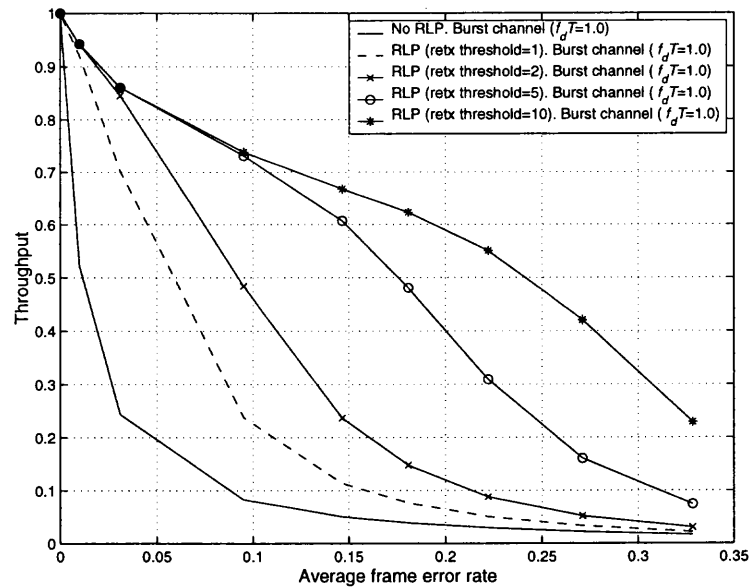

Figure 6.8 TCP throughput of system with RLP in data link layer (less correlated channel with $f_d T = 1.0$). The results approach that on independent channel.
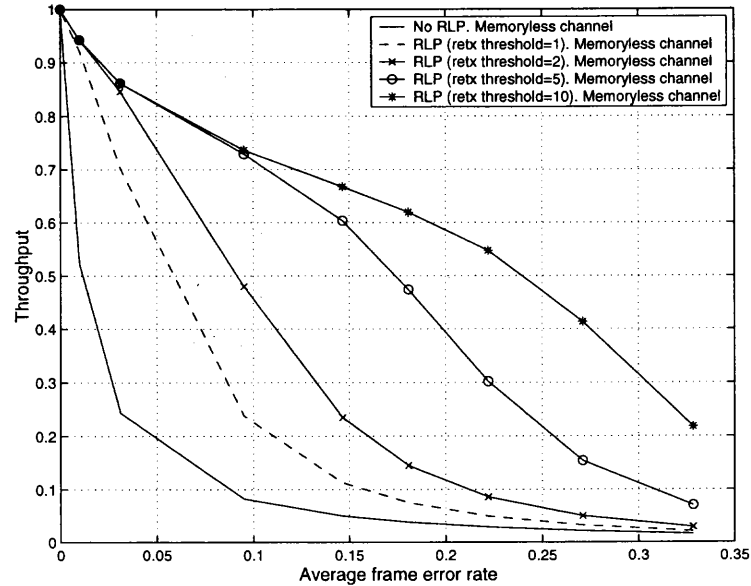
Figure 6.9 TCP throughput of system with RLP in data link layer (independent channel)

One can see the *cwnd* in system without RLP shrinks frequently with each error detected. For system with RLP, as more errors corrected by RLP and less errors seen by TCP layer, the *cwnd* shrinks less frequently. This means higher throughput is achieved.

6.3.3 Performance Comparison of TCP/ARQ and TCP/JARQ Protocols

Among the introduced wireless TCP approaches, the TCP/IP header compression scheme and SACK scheme are approaches supplementing the TCP protocol. They can be integrated with other wireless TCP approaches, like the split-connection protocol, snoop protocol, ELN, and link layer protocol. This section compares these approaches by summarizing the simulation results in [69] and presenting the performance of the proposed wireless TCP link layer approach, i.e., TCP/JARQ protocol.

The main advantage of the split-connection approach is that they isolate the TCP source from wireless losses. The retransmissions are performed by the TCP sender of the second wireless connection in case of error. The disadvantage of this
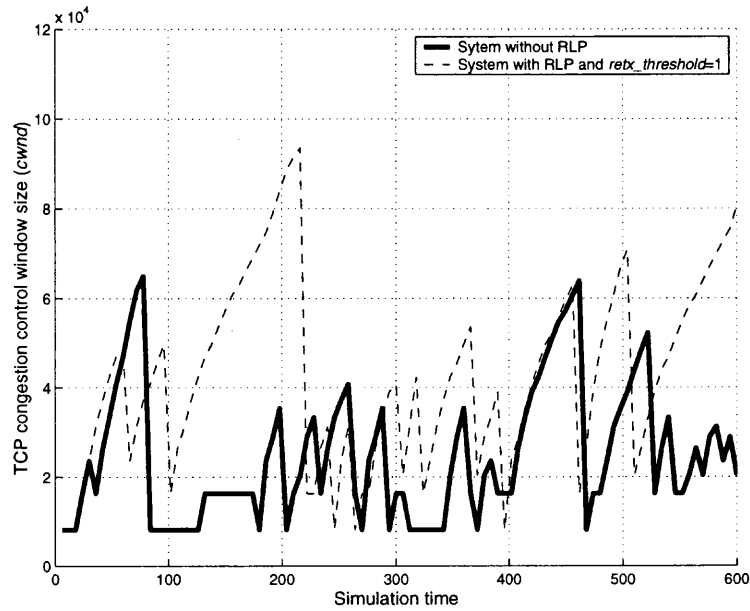
Figure 6.10 Comparison of TCP congestion window size *cwnd* of system without RLP and system with RLP and 1 retransmission attempt ($retx\_threshold = 1$)

Figure 6.11 Comparison of TCP congestion window size *cwnd* of system without RLP and system with RLP and 10 retransmission attempts ($retx\_threshold = 10$)

approach is TCP layer may often shrink its congestion control window or time out because the TCP layer is not well tuned for the lossy link. In addition, it maintains a significant amount of state per TCP connection and handoff process may tend to be complicated and slow.

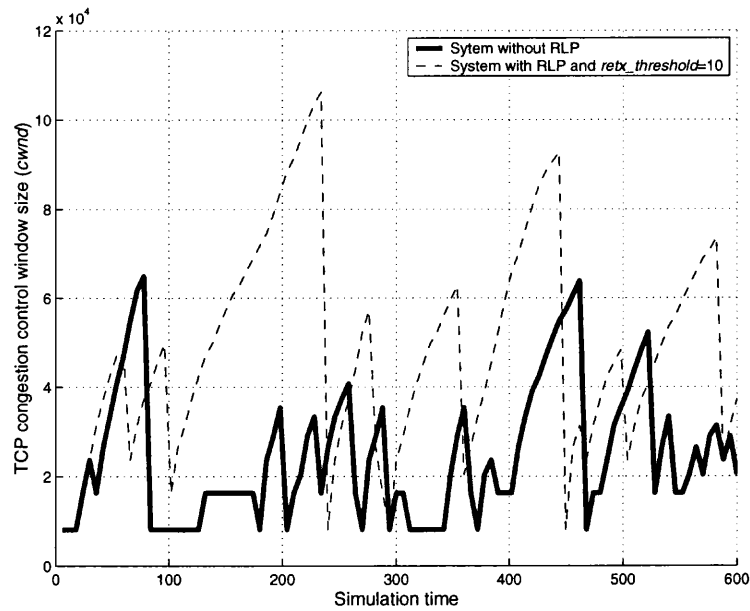The ELN protocol adds an explicit loss notification option to TCP acknowledgments when a packet is dropped due to the error, future acknowledgments corresponding to the lost packet are marked to tell the TCP sender that the error is caused by link error, not the congestion. Thus TCP may perform retransmission without invoking congestion control and avoidance algorithm. Thus the throughput is improved by preventing unnecessary fluctuation in the transmission window.

The link layer protocol fits naturally into the wireless TCP structure and operates independently of higher layers protocols. It does not maintain any per-connection state. The 200 ms TCP timeout granularity allows the link layer to perform several retransmission attempt to correct error locally. The disadvantage of link layer protocol is that the TCP layer may not be fully shielded from the packet loss and it may fast retransmit the packet that are locally retransmitted. The snoop protocol can be classified as a link layer protocol.

The simulation results in [69] show that the link layer has best performance among these approaches, with over 30% higher throughput than the split-connection approach, and over 20% higher than ELN approach. Link layer protocol with TCP awareness and SACK may achieve even better performance. Actually, the digital cellular systems, CDMA and TDMA, uses link layer approach with ARQ schemes. With JARQ protocol, a better throughput is expected to achieve.

Figure 6.12 shows a comparison of TCP throughput using ARQ and JARQ protocol on independent channel. Throughputs for system without RLP, system using RLP with retransmission ratio equaling to 1 and 2 are simulated, respectively. It is clear that at low frame error rate, JARQ outperforms conventional ARQ

schemes because of its larger code rate. However, as frame error rate increases, the detriment of retransmitting extra packets becomes more than the code rate gain and the performance of JARQ degrades more than that of the conventional ARQ schemes.
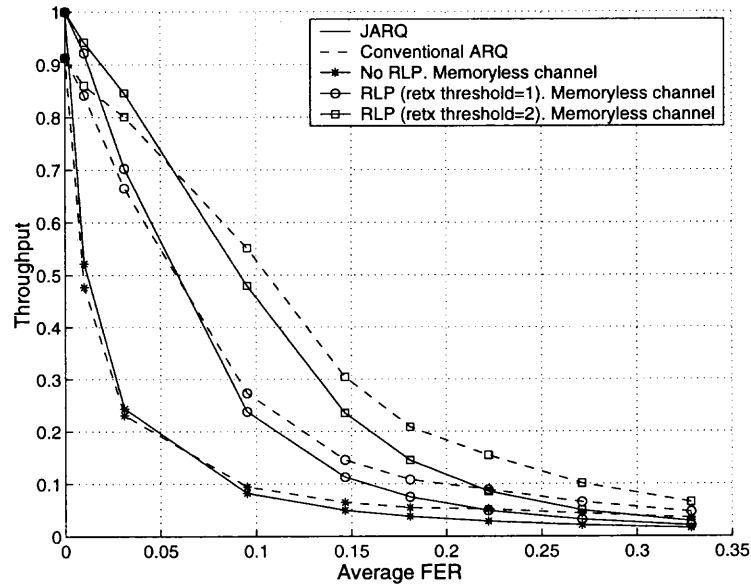
Figure 6.12 Simulation comparison of system using JARQ and conventional ARQ schemes

Although the figure shows the persistence at the RLP layer can improve system performance in the simulation, it is not always true. It is shown that in a multiple access scenario, longer persistence would degrade system performance especially when the channel is correlated [52, 86].

6.4 Summary

Since the TCP protocol is well tuned in channel with low error rate, in a lossy wireless environment, JARQ is introduced in data link layer to improve the performance of wireless TCP networks. Simulation results show the persistent retransmission in JARQ is beneficial to TCP layer because TCP layer would see fewer errors thus its congestion control and avoidance algorithm perform efficiently. Basically, the

more retransmission attempts, the fewer errors in higher layer and the better TCP throughput obtained. However, the persistence in RLP of data link layer would degrade system performance in some cases.

CHAPTER 7

JARQ APPLICATION TO REAL-TIME TRANSMISSION WITH LIMITED NUMBER OF RETRANSMISSION

In some systems needing a certain QoS, the traditional separate design often fails. The joint source and channel design is developed to maximize throughput while trying to guarantee a satisfactory QoS. This chapter discusses the application of JARQ protocol to real-time transmission, taking MPEG video transmission as an example. To meet the timing requirement, the number of retransmissions is limited. Although the limited retransmission is not capable to correct all the errors, it is applicable to real-time transmission system because most of these systems can tolerate certain data damages.

7.1 Introduction

The basic idea of all ARQ protocols is to correct errors through persistent retransmissions. This is true also for JARQ which uses lossless compression and when error is detected, packet is retransmitted persistently until the error is corrected. Although the error would be corrected eventually, the persistent retransmission may introduce long delay thus ARQ protocol is not suitable for real-time transmission, such us video transmission.

To solve the problem, limited retransmission is proposed which limits the number of retransmissions in case of error to meet the real-time requirements. This work includes the QSR-ARQ proposed by Wang *et al.* [78], where the ARQ protocol is QoS aware. It also applies limited retransmission by simulating the performance of video transmission and analyzing delay property of the approach, as well. The limited number of retransmissions may get packet lost but in fact, some of the real-time applications, such as video transmission, can tolerate certain data damages. Instead, timing is a crucial requirement for comfortable viewing. In particular, the

layered structure in MPEG [87, 88] make this approach applicable to real-time video transmission.

In the rest part of this chapter, JARQ protocol is applied to MPEG transmission and discuss the delay property of different number of retransmission. Three frame types in MPEG is introduced in Section 7.2. These different frame types have different timing requirements. In Section 7.3, the delay property of different number of retransmissions is analyzed by using signal flow graph. To verify the analysis, the mean delay of correctly transmitting one packet is obtained by summing all the probabilities of retransmission and hence obtain the same throughput as that in Chapter 4. The MPEG frames are classified as three categories and apply JARQ protocol with different tolerance to them. The packet delay and delay standard deviation are simulated in Section 7.4. Final section draws some conclusions.

7.2   Three Frame Types in Layered MPEG Application

MPEG is a layered encoded video application and it has two main functions: on one hand the quality requirements demand a very high compression ratio; on the other hand, random access requires that a compressed video bit stream be accessible in its middle and any frames of video be decodable in a limited amount of time.

Because of the importance of random access for stored video and the significant bit rate reduction afforded by motion-compensated interpolation, three types of frames are considered in MPEG, i.e., an intra coded frame (I-frame), a predictive coded frame (P-frame), and a bi-directionally predictive coded frame (B-frame). Intra coded frame provides access points for random access but only with moderate compression; predictive coded frame is coded with reference to a past frame (intra coded or predictive coded frame) and will in general be used as a reference for future predictive coded frames; bi-directionally predictive coded frame provides the highest amount of compression but requires both a past and a future reference for prediction.

Bi-directionally predictive coded frame is never used as reference. In all cases when a picture is coded with respect to a reference, motion compensation is used to improve the coding efficiency. The relationship between the three frame types is illustrated in Figure 7.1. The organization of the pictures in MPEG is quite flexible and will depend on application-specific parameters such as random accessibility and coding delay. As an example in Figure 7.1, an intra coded frame is inserted every 8 frames, and the ratio of bi-directionally predictive coded frame to intra coded or predictive coded frame is three out of four. Another type of data, the header which a video sequence always starts with, holds the important control information, such as the picture size, the image data start position and the Group of Picture (GOP) structure, etc.

Forward Prediction

Bidirectional Prediction
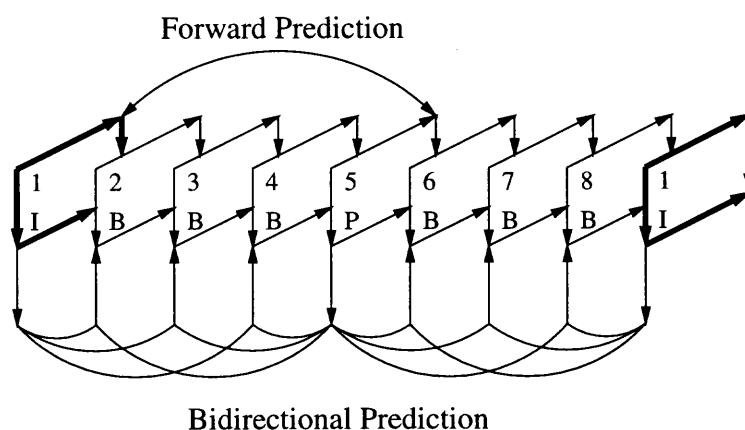
Figure 7.1 Three MPEG frame types

Since these frames have different timing requirements, to apply ARQ protocol, they can be classified into three classes according to their significances. The most important data, such as the frame header, should use basic JARQ with persistent retransmission. Some important data, such as I- and P-frame, use JARQ with limited number of retransmissions to achieve timing guarantee and low probability of data loss. The data needing only the timing requirement, such as B-frame, does not apply ARQ at all. It is transmitted only once.

Obviously, the second data class is of interest here. The delay and delay variance is about to be found using JARQ with limited number of retransmissions in simulation results.

7.3 Delay Analysis of Different Number of Retransmission

The throughput of JARQ protocol is analyzed by using signal flow graph in Chapter 4. It shows that the throughput changes with q^{M+1} where q is the probability of correct packet and M is the number of more retransmissions in case of error. M is small, i.e., 1 or 2, for most applications.

This section analyzes the delay property of different number of retransmissions by using signal flow graph. To verify the analysis, the mean delay of correctly transmitting one packet is obtained by summing all the probabilities of retransmission and hence obtain the same throughput as that in Chapter 4. Go-Back-(N, M) with $M = 1$ is used for example. The signal flow graph is shown in Figure 7.2.
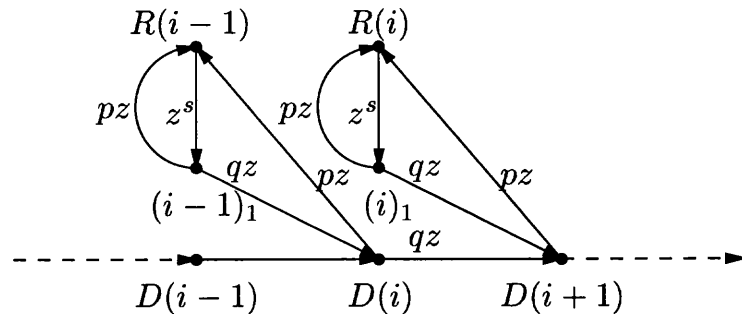
Figure 7.2 Signal flow graph of Go-Back-(N, M) protocol $(M = 1)$

Since the flow is similar for reach retransmission, the retransmission of ith packet at node $D(i)$ is analyzed. For i^{th} packet, it may be either correct with probability q and state transfers from node $D(i)$ to node $D(i + 1)$, or incorrect with probability $p = 1 - q$ and retransmission starts from packet $i - 1$ at node $R(i - 1)$. After a round-trip delay, denoted by $s + 1$, packet $i - 1$ is checked at node $(i - 1)_1$. If

it is correct, packet i is retransmitted and checked at $D(i)$. Otherwise, packet $i-1$ is retransmitted and checked again at node $(i-1)_1$.

If packet is correct at node $D(i)$ for the first time, then the delay is 1 (transmission delay of one packet) with probability q. If packet is initially incorrect but get corrected by one retransmission, then state flows through $D(i)$, $R(i-1)$, $(i-1)_1$, $D(i)$, and arrives at $D(i+1)$. The delay is $1+s+1+1 = (s+1)+2$ with probability $p \times q \times q = pq \times q$. If packet is retransmitted twice, one may see this state flow: $D(i) \to R(i-1) \to (i-1)_1 \to R(i-1) \to (i-1)_1 \to D(i) \to D(i+1)$. The delay is $1+s+1+s+1+1 = 2(s+1)+2$ with probability $p \times p \times q \times q = pq \times p \times q$. This is the case that retransmission of $(i-1)^{\text{th}}$ packet is incorrect but the retransmission of ith packet is correct. Another case is that retransmission of $(i-1)^{\text{th}}$ packet is correct but the retransmission of ith packet is incorrect. The delay for this case is $2(s+2)+1$ with probability $(pq)^2 \times q$.

To account for all the probabilities, the delay until a packet is correctly transmitted is summarized as follows.

$$D_{ij} = j[1+1+i(s+1)]+1, \qquad (7.1)$$

with probability $(pq \times p^i)^j \times q$ for $0 < i < \infty$ and $0 < j < \infty$. Thus from Eq.(7.1), it is possible to determine the delay for given s.

To verify the derivation, mean delay of correctly transmitting one packet is calculated. First, all the probabilities is summed,

$$\begin{aligned}
\sum_{j=0}^{\infty} \left(pq \sum_{i=0}^{\infty} p^i \right)^j \times q &= \sum_{j=0}^{\infty} \left(pq \times \frac{1}{1-p} \right)^j \times q \\
&= \sum_{j=0}^{\infty} p^j \times q \\
&= \frac{1}{1-p} \times q = 1. \qquad (7.2)
\end{aligned}$$

Next, the mean delay is calculated,

$$
\begin{aligned}
\overline{D} &= q \times \sum_{j=0}^{\infty} p^j \left\{ j \times \left[(s+1)q \sum_{i=0}^{\infty} (i+1)p^i + 1 \right] + 1 \right\} \\
&= q \times \sum_{j=0}^{\infty} p^j \times \left[j \left(\frac{s+1}{q} + 1 \right) + 1 \right] \\
&= q \times \left(\frac{s+1+q}{q} \times \frac{p}{q^2} + \frac{1}{q} \right) \\
&= \frac{1+ps}{q^2}.
\end{aligned}
\tag{7.3}
$$

Thus the throughput is

$$
\eta_{\text{gbnm } (M=1)} = \frac{1}{\overline{D}} = \frac{q^2}{1+ps}.
\tag{7.4}
$$

This is the same result that is obtained from Eq.(4.4) in Chapter 4 with $M = 1$. The throughput for $M > 1$ can also be verified with similar derivation.

7.4 Simulations

Three types of data in Section 7.2 are classified. Since the delay and delay variance of JARQ with limited number of retransmissions are of interest, details of the MPEG encoding and decoding algorithm are not considered. In stead, one frame is selected from the video sequence *Top Gun* as packet to be transmitted in the simulation.

The frame (packet) delay of different number of retransmissions are shown in Figure 7.3 to Figure 7.5. These figures compare the delay between basic JARQ (persistent retransmission) and JARQ with limited retransmission. Retransmission limit equals to 1, 2, and 3, respectively. Assuming that the time to transmit one packet is 1, the round-trip delay is $s = 5$. The packet error rate is 0.3 in these figures. The figure shows that basic JARQ may lead to a large delay (65 in the figure). In Figure 7.3, 1 retransmission is allowed. One may see following values of delay. One means that packet is correct for the first time. Seven means both the transmission and retransmission are incorrect and after 1 retransmission $(1 + 5 + 1 = 7)$, the

JARQ fails to correct error and the data is damaged. 8 means the erroneous packet is corrected by first retransmission and the delay is $1 + 5 + 1 + 1 = 8$.

Similarly for the case of two retransmission attempts in Figure 7.4, the delays are 1, 8, 13, 14, and 15. The delay of the case of three retransmission attempts can be determined as well.

Figure 7.3 Comparison of packet delay of basic JARQ and JARQ with retransmission limit equal to 1. Packet error rate is 0.3.

The standard deviation of the delay is shown in Figure 7.6 (the variance is the square of standard deviation). It is clear that the smaller retransmission limit, the better deviation. This is because for small retransmission limit, the number of delay values is few. For large retransmission limit, the delay is chosen from large range of values.

Although a good delay and delay variance property of limited retransmission are achieved, the price is that packet may suffer high error rate. The percentage of correct packet versus number of retransmissions is plotted in Figure 7.7. Packet error rates of 0.1, 0.2, 0.3, and 0.4 are studied. The results show that not only the number of correct packet increases with number of retransmissions, it also increases fast,
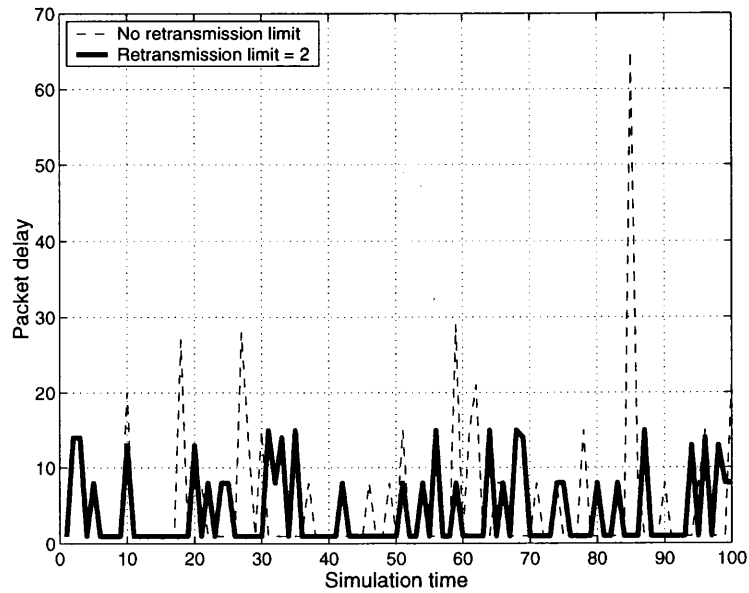
Figure 7.4 Comparison of packet delay of basic JARQ and JARQ with retransmission limit equal to 2. Packet error rate is 0.3.

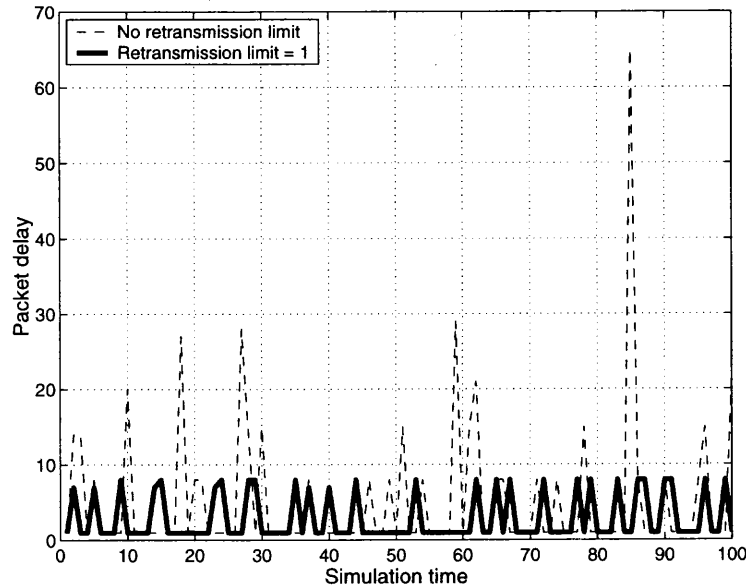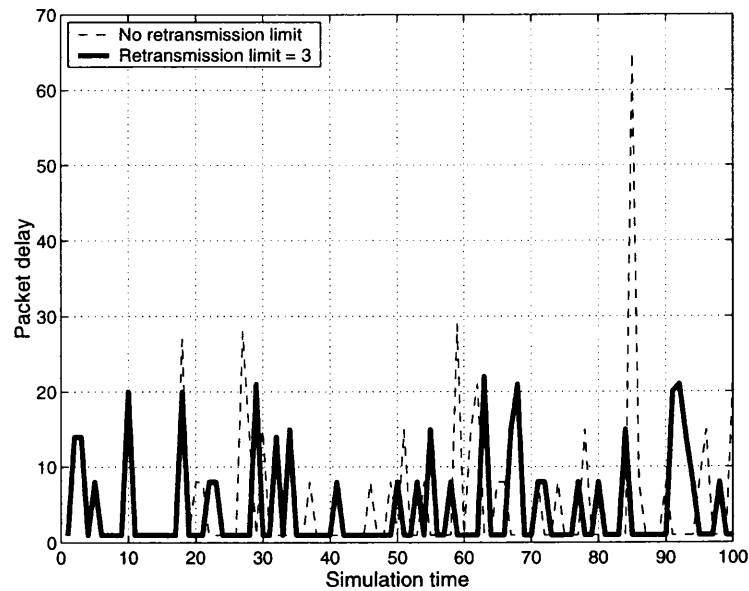**Figure 7.5** Comparison of packet delay of basic JARQ and JARQ with retransmission limit equal to 3. Packet error rate is 0.3.
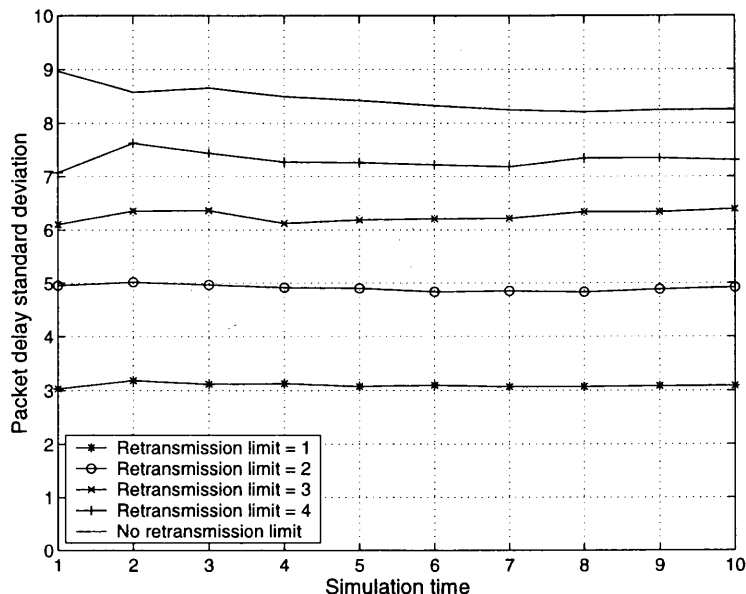
Figure 7.6 Comparison of packet delay standard deviation of basic JARQ and JARQ with retransmission limit equal to 1, 2, 3, and 4, respectively. Packet error rate is 0.3.

especially for small packet error rate case. For example, when packet error rate is 0.1, Figure 7.7 shows that one retransmission can correct almost all the errors. This means JARQ protocol with limited retransmission is applicable to video transmission by providing a low probability of data loss while achieving a satisfactory QoS.
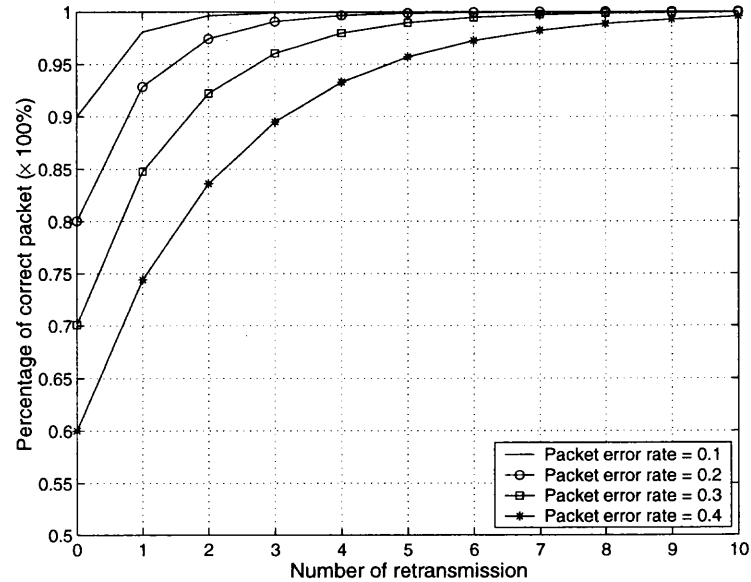
Figure 7.7 Percentage of correct packet of different number of retransmissions. Packet error rate is 0.1, 0.2, 0.3 and 0.4, respectively.

7.5 Conclusion

The JARQ protocol is applied to real-time transmission by limiting the number of retransmissions to meet the timing requirement. The delay of different number of retransmissions limit is analyzed and the analysis is validated by achieving the same throughput in Chapter 4. The simulation result shows that not only a good delay and delay variance property are obtained by the limited retransmission, but also most errors can be corrected by a small number of retransmissions. It concludes that the JARQ protocol with limited retransmission is applicable to real-time transmission by providing a low probability of data damage while achieving a satisfactory QoS.

CHAPTER 8
CONCLUSIONS AND FUTURE WORK

This dissertation is divided into three parts. First, a joint source and channel design with arithmetic coding is proposed. The self-synchronization property of arithmetic codes is used to detect error, but error propagation may be introduced. Next, the proposed joint source and channel design is applied to communication networks and the error recovery protocol is introduced for the design. The error propagation may introduce delay detection and a JARQ protocol, i.e., Go-Back-(N, M) protocol, is proposed which accepts the current packet as correct only when the following M packets are correct, as well. The performance of the protocol on both independent channel and nonindependent channels are analyzed by using signal flow graph. Finally, two applications of the JARQ protocol are discussed, one is a TCP/JARQ protocol stack for wireless TCP networks and the other is JARQ with limited number of retransmissions for real-time transmission.

In the joint source and channel design, the self-synchronization property of arithmetic codes is used to detect error, but the price is error propagation is introduced. The error propagation distance PDF is discussed and modeled for both text and image transmission. It is found that there are few errors which propagate for long distance. The arithmetic coding with adaptive algorithm is analyzed and two types of error are found. To detect these errors, two different marker strategies are introduced. Simulation result shows that this scheme is capable of detecting error with small delay, which gives us more code rate and throughput in communication networks.

A comparison of the error detection capability is presented between the marker symbol approach and the forbidden symbol approach of other work. It shows two approaches have basically the same error detection capability. The difference is that the forbidden symbol approach is efficient in error correction because its geometric

distribution of error propagation distance allows estimation of error location. The marker symbol approach is simple and a better choice in packet switching networks where the complexity of high frequency of error checking in forbidden symbol approach is generally not needed.

In the use of the proposed design in communication networks, an error recovery scheme called JARQ protocol is presented for transmission of compressed data over packet switching networks. Since it is possible that the error detection process encounters some delay, A Go-Back-(N, M) protocol is used where the receiver accepts the current packet as correct only when the following M packets are correct, as well. Taking the advantage of nonuniform error propagation distance PDF, the receiver can estimate the error location and perform packet combining. A second retransmission is often avoided and system performance is improved.

The throughput of JARQ protocol is analyzed for both independent channel and nonindependent channels by using signal flow graph. Due to the delayed detection, the throughput is dropped to the order of number of extra retransmissions. However, this impact is alleviated when BER is small. At high BER's, packet combining is introduced and significant throughput gain is achieved. On nonindependent channel, a good performance can be obtained at high correlation (at small normalized Doppler bandwidth $f_d T$). The throughput decreases when the channel becomes less correlated, i.e., more independent (at large $f_d T$), and approaches the throughput on the independent channel. In addition, The throughput is increased with a larger code rate, compared with conventional ARQ scheme. The simulation result validate the analysis.

As one of the application of JARQ protocol, a TCP/JARQ protocol stack is proposed for wireless TCP networks because joint source and channel design is crucial for wireless communications system to achieve optimal performance. Since the TCP protocol is well tuned in channel with low error rate, in a lossy wireless

environment, JARQ is introduced in data link layer to improve the performance of wireless TCP networks. Simulation results show the persistent retransmission in JARQ is beneficial to TCP layer because TCP layer would see fewer errors thus its congestion control and avoidance algorithm perform efficiently. Basically, the more retransmission attempts, the fewer errors in higher layer and the better TCP throughput obtained.

Another application of JARQ protocol is to apply it to real-time transmission by limiting the number of retransmissions to meet the timing requirement. The delay of different number of retransmissions limit is analyzed. Simulation result shows that not only a good delay and delay variance property are obtained by the limited retransmission, but also most errors can be corrected by a small number of retransmissions. It concludes that the JARQ with limited retransmission is applicable to real-time transmission by providing a low probability of data damage while achieving a satisfactory QoS.

In addition to the coverage in this dissertation of introducing a new joint source and channel design, analyzing the error recovery protocol, and applying the design to communications systems, following issues should be further studied.

1. Integration of the proposed work with other joint source and channel coding schemes. The study of the proposed scheme in this dissertation focuses on the introduction of marker symbol strategy and analyzing error propagation distance PDF. One important issue of lots of other joint source and channel design approaches is how to allocate the best code rate so the optimal channel use is obtained. Although it is possible to modify the source distributions to produce a code word with any information rate [14], and the code rate can be changed by applying different marker block length, the relationship between this length and the optimal code rate should be investigated.

2. The implementation of packet combining. The idea of packet combining is proposed. How to implement packet combining is a further study topic. This includes the selection of buffer size, computation complexity, processing delay, and the trade off among them. Note that the packet combining can be applied to a packet (intra packet combining) or to a frame containing several packets (inter packet combining). The implementation of these two cases should be studied.

3. The computation complexity and comparison of existing systems in terms of timing requirements. Some communications systems require strict timing conditions, especially in wireless communication networks where system resources are limited. An example is for 3G wireless links, the Turbo decoder (the de-interleaver) requires as much as 20 ms of processing time.

   Although it is hard to compare a JARQ system to an equivalent above system with same error detection/correction capability and system performance, etc., a simple explanation of computation complexity of two systems may be insightful. Eq.(2.11) to Eq.(2.14) show that in JARQ system, only several additions and multiplications are carried out during encoding and decoding, which are much simpler than iterative computation of Turbo codes. Note that a marked block of bytes have to be calculated in JARQ system to detect an error, while in conventional ARQ systems, data also come in block to be decoded. The size of two systems are comparable and this implies that the computation complexity of JARQ is much less.

   However, to draw a more accurate comparison, the computation complexity of these systems should be further studied.

4. Applications of the JARQ protocol. Two applications of JARQ protocol are presented in this work. The study of TCP/JARQ protocol should be extended

to integrate JARQ with other wireless TCP approaches like SACK and ELN. By making TCP aware of the error, the throughput can be further improved. In the study of JARQ with limited number of retransmission, the MPEG encoding and decoding process are not supported in Chapter 7 and to make the work more applicable, they should be considered in further study.

Other applications should be also introduced. These may include the medical image transmission which requires a lossless image transmission. The JARQ protocol, based on lossless source and channel coding, may improve the performance of this application. This should be further investigated.

REFERENCES

1. C. E. Shannon, "A mathematical theory of communication," *Bell Syst. Tech. J.*, vol. 27, pp. 379–423, 623–656, July 1948.

2. S. Vembu, S. Verdú, and Y. Steinberg, "The source-channel separation theorem revisited," *IEEE Trans. Inform. Theory*, vol. 41, pp. 44–54, Jan. 1995.

3. M. E. Hellman, "On using natural redundancy for error detection," *IEEE Trans. Commun.*, vol. 22, pp. 1690–1693, Oct. 1974.

4. J. W. Modestino, V. Bhaskaran, and J. B. Anderson, "Tree encoding of images in the presence of channel errors," *IEEE Trans. Inform. Theory*, vol. 27, pp. 667–697, Nov. 1981.

5. A. Goldsmith, "Joint source/channel coding for wireless channels," in *Proceedings of the IEEE Vehicular Technology Conference*, (Chicago, IL), pp. 614–618, July 1995.

6. V. Kafedziski and D. Morrell, "Joint source channel coding over frequency selective fading channels with feedback using OFDM," in *Proceedings of the IEEE Vehicular Technology Conference*, (Phoenix, AZ), pp. 1390–1394, May 1997.

7. B. Masnick and J. Wolf, "On linear unequal error protection codes," *IEEE Trans. Inform. Theory*, vol. 13, pp. 600–607, Oct. 1967.

8. R. H. Morelos-Zaragoza, M. P. C. Fossorier, S. Lin and H. Imai, "Multilevel coded modulation for unequal error protection and multistage decoding—Part I: Symmetric constellations," *IEEE Trans. Commun.*, vol. 48, pp. 204–213, Feb. 2000.

9. M. Isaka, M. P. C. Fossorier, R. H. Morelos-Zaragoza, S. Lin and H. Imai, "Multilevel coded modulation for unequal error protection and multistage decoding—Part II: Asymmetric constellations," *IEEE Trans. Commun.*, vol. 48, pp. 774–786, May 2000.

10. K. Sayood and J. C. Borkenhagen, "Use of residual redundancy in the design of joint source/channel coders," *IEEE Trans. Commun.*, vol. 39, pp. 838–846, June 1991.

11. K. Sayood, H. H. Otu, and N. Demir, "Joint source/channel coding for variable length codes," *IEEE Trans. Commun.*, vol. 48, pp. 787–794, May 2000.

12. T.-C. Yang, S. Kumar, and C.-C. J. Kuo, "Robust image compression based on self-synchronizing Huffman code and inter-subband dependency," in *Proceedings of the Thirty-Second Asilomar Conference on Signals, Systems and Computers*, (Monterey, CA), pp. 1631–1635, Nov. 1998.

13. C. Boyd, J. G. Cleary, S. A. Irvine, I. Rinsma-Melchert, and I. H. Witten, "Integrating error detection into arithmetic coding," *IEEE Trans. Commun.*, vol. 45, pp. 1–3, Jan. 1997.

14. J. Sayir, "Arithmetic coding for noisy channels," in *Proceedings of the 1999 IEEE Information Theory and Communications Workshop*, (Kruger National Park, South Africa), pp. 69–71, June 1999.

15. G. F. Elmasry, "Arithmetic coding algorithm with embedded channel coding," *Electronic Letters*, vol. 33, pp. 1687–1688, Sept. 1997.

16. G. F. Elmasry, "Joint lossless-source and channel coding using automatic repeat request," *IEEE Trans. Commun.*, vol. 47, pp. 953–955, July 1999.

17. G. G. Langdon, Jr., "An introduction to arithmetic coding," *IBM J. Res. Develop.*, vol. 28, pp. 135–149, Mar. 1984.

18. P. G. Howard and J. S. Vitter, "Arithmetic coding for data compression," in *Proceedings of the IEEE*, pp. 857–865, June 1994.

19. A. Moffat, R. Neal, and I. H. Witten, "Arithmetic coding revisited," in *Proceedings of the Data Compression Conference*, (Snowbird, UT), pp. 202–211, Mar. 1995.

20. P. G. Howard and J. S. Vitter, "Analysis of arithmetic coding for data compression," in *Proceedings of the Data Compression Conference*, (Snowbird, UT), pp. 3–12, Apr. 1991.

21. B. D. Pettijohn, K. Sayood, and M. W. Hoffman, "Joint source/channel coding using arithmetic codes," in *Proceedings of the Data Compression Conference*, (Snowbird, UT), pp. 73–82, Mar. 2000.

22. I. Kozintsev, J. Chou, and K. Ramchandran, "Image transmission using arithmetic coding based continuous error detection," in *Proceedings of the Data Compression Conference*, (Snowbird, UT), pp. 339–348, Mar.–Apr. 1998.

23. B. He, G. F. Elmasry, C. N. Manikopoulos, and Y.-Q. Shi, "A Go-Back-$N + 1$ protocol and its application in wireless ATM networks," in *Proceedings of the 33rd Annual Conference on Information Sciences and Systems*, (Baltimore, MD), Mar. 1999.

24. B. He and C. N. Manikopoulos, "An automatic repeat request protocol using joint source and channel coding," in *Proceedings of the CSCC 2000 World Multiconference*, (Athens, Greece), July 2000.

25. C. B. Jones, "An efficient coding system for long source sequences," *IEEE Trans. Inform. Theory*, vol. 27, pp. 280–291, May 1981.

26. W. H. Press, S. A. Teukolsky, W. T. Vetterling, and B. P. Flannery, *Numerical Recipes in C: The Art of Scientific Computing*. Cambridge, MA: Cambridge University Press, 2nd ed., 1992.

27. B. He and C. N. Manikopoulos, "A comparison between two error detection techniques using arithmetic coding," in *Proceedings of the Data Compression Conference*, (Snowbird, Utah), Mar. 2001.

28. B. He and C. N. Manikopoulos, "A comparison between two error detection techniques using arithmetic coding," in *to appear in Proceedings of the International Conference on Computing and Information Technologies*, (Upper Montclair, NJ), Oct. 2001.

29. S. Lin and D. J. Costello, Jr., *Error Control Coding: Fundamentals and Applications*. Englewood Cliffs, NJ: Prentice-Hall, Inc., 1985.

30. A. S. Tanenbaum, *Computer Networks*. Upper Saddle River, NJ: Prentice-Hall, Inc., 3rd ed., 1996.

31. M. Schwartz, *Telecommunication Networks: Protocols, Modeling and Analysis*. Reading, MA: Addison-Wesley Publishing Company, 1988.

32. B. He, G. F. Elmasry and C. N. Manikopoulos, "Joint lossless-source and channel coding using ARQ/Go-Back-(N, M) for image transmission," submitted to *the IEEE Trans. Image Processing*, 2000.

33. B. He and C. N. Manikopoulos, "ARQ protocols for joint lossless-source and channel coding with delayed detection," submitted to *the IEEE Trans. Commun.*, 2000.

34. B. He, G. F. Elmasry and C. N. Manikopoulos, "A network protocol for joint lossless-source and channel coding (JARQ) with packet combining," in *Proceedings of the 34th Annual Conference on Information Sciences and Systems*, (Princeton, NJ), Mar. 2000.

35. A. M. Y. Bigloo, T. A. Gulliver, and V. K. Bhargava, "Maximum-likelihood decoding and code combining for DS/SSMA slotted aloha," *IEEE Trans. Commun.*, vol. 45, pp. 1602–1612, Dec. 1997.

36. J. J. D'Azzo and C. H. Houpis, *Linear Control System Analysis and Design: Conventional and Modern*. New York, NY: McGraw-Hill, Inc., 2nd ed., 1981.

37. D.-L. Lu and J.-F. Chang, "Analysis of ARQ protocols via signal flow graphs," *IEEE Trans. Commun.*, vol. 37, pp. 245–251, Mar. 1989.

38. D. P. Bertsekas and R. G. Gallager, *Data Networks*. Englewood Cliffs, NJ: Prentice-Hall, Inc., 2nd ed., 1992.

39. B. He and C. N. Manikopoulos, "Performance analysis of ARQ protocol with delayed detection for joint source and channel coding," in *Proceedings of the 35th Annual Conference on Information Sciences and Systems*, (Baltimore, MD), Mar. 2001.

40. D. E. Mcdysan and D. L. Spohn, *ATM Theory and Application*. New York, NY: McGraw-Hill, Inc., 1995.

41. E. N. Gilbert, "Capacity of a burst-noise channel," *Bell Syst. Tech. J.*, vol. 39, pp. 1253–1265, Sept. 1960.

42. B. D. Fritchman, "A binary channel characterization using partitioned Markov chains," *IEEE Trans. Inform. Theory*, vol. 13, pp. 221–227, Apr. 1966.

43. L. N. Kanal and A. R. K. Sastry, "Models for channels with memory and their applications to error control," in *Proceedings of the IEEE*, vol. 66, pp. 724–744, July 1978.

44. H. S. Wang and P.-C. Chang, "On verifying the first-order Markovian assumption for a Rayleigh fading channel model," *IEEE Trans. Veh. Technol.*, vol. 45, pp. 353–357, May 1996.

45. A. Abdi, "Comments on 'On verifying the first-order Markovian assumption for a Rayleigh fading channel model'," *IEEE Trans. Veh. Technol.*, vol. 48, p. 1739, Sept. 1999.

46. M. Zorzi, R. R. Rao, and L. B. Milstein, "On the accuracy of a first-order markov model for data transmission on fading channels," in *Proceedings of the IEEE International Conference on Universal Personal Communications*, (Tokyo, Japan), pp. 211–215, 1995.

47. E. O. Elliott, "Estimates of error rates for codes on burst-noise channels," *Bell Syst. Tech. J.*, vol. 42, pp. 1977–1997, Sept. 1963.

48. R. Krishnan and J. A. Silvester, "Resource allocation in broadband networks-cell, burst or connection level?," in *Proceedings of the IEEE International Conference on Communications*, (New Orleans, LA), pp. 86–90, May 1994.

49. H. Michiel and K. Laevens, "Teletraffic engineering in a broad-band era," in *Proceedings of the IEEE*, vol. 85, pp. 2007–2033, Dec. 1997.

50. R. G. Garroppo, S. Giordano, M. Pagano, and G. Procissi, "On the relevance of correlation dependencies in ON/OFF characterization of broadband traffic," in *Proceedings of the IEEE International Conference on Communications*, (New Orleans, LA), pp. 811–815, June 2000.

51. M. Zorzi, R. R. Rao, and L. B. Milstein, "Error statistics in data transmission over fading channels," *IEEE Trans. Commun.*, vol. 46, pp. 1468–1477, Nov. 1998.

52. A. Chockalingam and G. Bao, "Performance of TCP/RLP protocol stack on correlated fading DS-CDMA wireless links," *IEEE Trans. Veh. Technol.*, vol. 49, pp. 28–33, Jan. 2000.

53. J. G. Kemeny and J. L. Snell, *Finite Markov Chains*. New York: Springer-Verlag, 1976.

54. J. G. Proakis and M. Salehi, *Communication Systems Engineering*. Englewood Cliffs, NJ: Prentice-Hall, Inc., 1994.

55. Y. J. Cho and C. K. Un, "Performance analysis of ARQ error controls under Markovian block error pattern," *IEEE Trans. Commun.*, vol. 42, pp. 2051–2061, Feb./Mar./Apr. 1994.

56. D.-L. Lu and J.-F. Chang, "Performance of ARQ protocols in nonindependent channel errors," *IEEE Trans. Commun.*, vol. 41, pp. 721–730, May 1993.

57. M. Zorzi and R. R. Rao, "Performance of ARQ Go-Back-N protocol in Markov channels with unreliable feedback: Delay analysis," in *Proceedings of the IEEE International Conference on Universal Personal Communications*, pp. 481–485, 1995.

58. J. C. I. Chuang, "Comparison of two ARQ protocols in a Rayleigh fading channel," *IEEE Trans. Veh. Technol.*, vol. 39, pp. 367–373, Nov. 1990.

59. B. He and C. N. Manikopoulos, "Performance of an ARQ protocol based on joint source and channel coding on nonindependent channel," in *to appear in Proceedings of the IEEE Vehicular Technology Conference (VTC-01/Fall)*, (Atlantic City, NJ), Oct. 2001.

60. B. He and C. N. Manikopoulos, "Performance analysis of ARQ protocols for joint lossless-source and channel coding with delayed detection," to be submitted to *the IEEE Trans. Commun.*, 2001.

61. B. He and C. N. Manikopoulos, "Efficient joint source and channel coding arq protocol for wireless networks," to be submitted to *the Electronic Letters*, 2001.

62. W. R. Stevens, *TCP/IP Illustrated, Volume 1: The Protocols*. Reading, MA: Addison-Wesley Publishing Company, 1994.

63. D. Comer, *Internetworking with TCP/IP, Volume 1: Principles, Protocols, and Architecture*. Upper Saddle River, NJ: Prentice-Hall, Inc., 3rd ed., 1995.

64. J. B. Postel, "Transmission control protocol," RFC 793, Information Sciences Institute, Marina del Rey, CA, Sept. 1981.

65. V. Jacobson, "Congestion avoidance and control," in *Proceedings of the ACM SIGCOMM'88 Conference*, (Stanford, CA), pp. 314–329, Aug. 1988. ftp://ftp.ee.lbl. gov/papers/congavoid.ps.Z.

66. V. Jacobson, "Modified TCP congestion avoidance algorithm," end2end-interest mailing list, Lawrence Berkeley National Laboratory, Aug. 1990. ftp://ftp.isi.edu/end2end/end2end-interest-1990.mail.

67. W. R. Stevens, "TCP slow start, congestion avoidance, fast retransmit, and fast recovery algorithms." RFC 2001, Jan. 1997. (Obsoleted by RFC 2581).

68. M. Allman, V. Paxson, and W. R. Stevens, "TCP congestion control." RFC 2581, Apr. 1999.

69. H. Balakrishnan, V. N. Padmanabhan, S. Seshan, and R. H. Katz, "A comparison of mechanisms for improving TCP performance over wireless links," *IEEE/ACM Trans. on Networking*, vol. 5, pp. 756–769, Dec. 1997.

70. G. Racherla, S. Radhakrishnan, and C. N. Sekharan, "Performance evaluation of wireless TCP schemes under different rerouting schemes in mobile networks," in *Proceedings of the 1998 IEEE TENCON'98*, vol. 1, (New Delhi, India), pp. 93–96, Dec. 1998.

71. K.-Y. Wang and S. K. Tripathi, "Mobile-end transport protocol: An alternative to TCP/IP over wireless links," in *Proceedings of the IEEE INFOCOM'98*, vol. 3, (San Francisco, CA), pp. 1046–1053, Mar.–Apr. 1998.

72. V. Jacobson, "Compressing TCP/IP headers for low-speed serial links." RFC 1144, Feb. 1990.

73. M. Degermark, M. Engan, B. Nordgren, and S. Pink, "Low-loss TCP/IP header compression for wireless networks," *Wireless Networks*, vol. 3, no. 5, pp. 375–387, 1998.

74. A. Bakre and B. R. Badrinath, "I-TCP: Indirect TCP for mobile hosts," in *Proceedings of the 15th International Conference on Distributed Computing Systems (ICDCS)*, (Vancouver, Canada), pp. 136–143, May–June 1995.

75. Z. J. Haas and P. Agrawal, "Mobile-TCP: An asymmetric transport protocol design for mobile systems," in *Proceedings of the IEEE International Conference on Communications*, vol. 2, (Montreal, Canada), pp. 1054–1058, June 1997.

76. H. Balakrishnan, S. Seshan, and R.H. Katz, "Improving reliable transport and handoff performance in cellular wireless networks," *ACM Wireless Networks*, vol. 1, pp. 469–481, Dec. 1995.

77. A. Chockalingam, M. Zorzi, and V. Tralli, "Wireless TCP performance with link layer FEC/ARQ," in *Proceedings of the IEEE International Conference on Communications*, (Vancouver, Canada), pp. 1212–1216, June 1999.

78. S. Wang, H. Zheng, and J. A. Copeland, "An error control design for multimedia wireless networks," in *Proceedings of the IEEE Vehicular Technology Conference*, vol. 2, (Tokyo, Japan), pp. 795–799, May 2000.

79. Y. Bai, A. T. Ogielski, and G. Wu, "Interactions of TCP and radio link ARQ protocol," in *Proceedings of the IEEE Vehicular Technology Conference*, vol. 3, (Amsterdam, The Netherlands), pp. 1710–1714, Sept. 1999.

80. F. Borgonovo, A. Capone, and L. Fratta, "Retransmissions versus FEC plus interleaving for real-time applications: A comparison between CDPA and MC-TDMA cellular systems," *IEEE J. Select. Areas Commun.*, vol. 17, pp. 2022–2030, Nov. 1999.

81. M. Mathis, J. Mahdavi, S. Floyd, and A. Romanow, "TCP selective acknowledgment options." RFC 2018, Oct. 1996.

82. TIA/EIA/IS-95, *Data Services Option Standard for Wideband Spread Spectrum Digital Cellular System*, May 1995.

83. TIA/EIA/IS-99, *Data Services Option Standard for Wideband Spread Spectrum Digital Cellular System*, July 1995.

84. TIA/EIA/IS-707, *Data Services Option Standard for Wideband Spread Spectrum Digital Cellular System*, Feb. 1998.

85. OPNET Modeler, © 2001 OPNET Technologies, Inc., Bethesda, MD. URL: http://www.opnet.com/.

86. A. Chockalingam, M. Zorzi, L. B. Milstein, and P. Venkataram, "Performance of a wireless access protocol on correlated Rayleigh-fading channels with capture," *IEEE Trans. Commun.*, vol. 46, pp. 644–655, May 1998.

87. D. LeGall, "MPEG: A video compression standard for multimedia applications," *Comm. ACM.*, vol. 34, pp. 46–58, Apr. 1991.

88. J. L. Mitchell, W. B. Pennebaker, C. E. Fogg, and D. J. LeGall, *MPEG video Compression Standard.* New York, NY: Chapman & Hall, 1997.